OPTIMAL COMBUSTION CONTROL OF UNTREATED LANDFILL GAS VIA AVERAGING PULSE WIDTH MODULATION

BY

MR. KANCHIT PAWANANONT

A DISSERTATION SUBMITTED IN PARTIAL FULFILLMENT OF THE REQUIREMENTS FOR THE DEGREE OF DOCTOR OF PHILOSOPHY (ENGINEERING AND TECHNOLOGY)
SIRINDHORN INTERNATIONAL INSTITUTE OF TECHNOLOGY
THAMMASAT UNIVERSITY
ACADEMIC YEAR 2021

OPTIMAL COMBUSTION CONTROL OF UNTREATED LANDFILL GAS VIA AVERAGING PULSE WIDTH MODULATION

BY

MR. KANCHIT PAWANANONT

A DISSERTATION SUBMITTED IN PARTIAL FULFILLMENT OF THE REQUIREMENTS FOR THE DEGREE OF DOCTOR OF PHILOSOPHY (ENGINEERING AND TECHNOLOGY)
SIRINDHORN INTERNATIONAL INSTITUTE OF TECHNOLOGY
THAMMASAT UNIVERSITY
ACADEMIC YEAR 2021

THAMMASAT UNIVERSITY
SIRINDHORN INTERNATIONAL INSTITUTE OF TECHNOLOGY

DISSERTATION

BY

MR. KANCHIT PAWANANONT

ENTITLED

OPTIMAL COMBUSTION CONTROL OF UNTREATED LANDFILL GAS VIA AVERAGING PULSE WIDTH MODULATION

was approved as partial fulfillment of the requirements for
the degree of Doctor of Philosophy (Engineering and Technology)

on November 9, 2021

Chairperson
(Associate Professor Pichaya Rachdawong, Ph.D.)

Member and Advisor
(Professor Thananchai Leephakpreeda, Ph.D.)

Member
(Assistant Professor Thunyaseth Sethaput, Ph.D.)

Member
(Assistant Professor Chung-Hao Hsu, Ph.D.)

Member
(Maroay Phlernjai, Ph.D.)

Director
(Professor Pruettha Nanakorn, D.Eng.)

Thesis Title	OPTIMAL COMBUSTION CONTROL OF UNTREATED LANDFILL GAS VIA AVERAGING PULSE WIDTH MODULATION
Author	Mr. Kanchit Pawananont
Degree	Doctor of Philosophy (Engineering and Technology)
Faculty/University	Sirindhorn International Institute of Technology/ Thammasat University
Thesis Advisor	Professor Thananchai Leephakpreeda, Ph.D.
Academic Years	2021

ABSTRACT

In Thailand, there have recently been a few small-scale preliminary studies on power generation from landfill gas so as to assess technical feasibility prior to performance of full-scale projects. This paper presents financial analysis of those studies on electricity generation by using an Internal Combustion Engine (ICE), Organic Rankine Cycle (ORC), Stirling Engine (STE). Financial indices, such as levelized cost of electricity, net present value, internal rate of return, and payback period, are determined from actual costs of those studies to produce electricity of the power engines from landfill gas. It is found that all financial indices of ICE are mostly acceptable compared with ORC and STE, although cost of gas preparation and high maintenance in ICE are required. From investigation, this advantage of ICE is because of the highest electricity generation with compactness and wide availability in local market. In turn, the levelized costs of electricity of ICE, ORC, and STE are 0.11 USD/kWh, 0.30 USD/kWh, 0.42 USD/kWh respectively. At present, ICE might be a promising engine until costs of the imported ORC and STE decrease at feasible level of finance.

The investment of landfill gas is still have high cost and by products (CH_4+CO_2). It should has a treatment process before using in the internal combustion engine for generating power. Therefore, this paper will present the external combustion by creating the system of untreated landfill gas. And the most important equipment for controlling this combustion is valve. In control of on–off valves for linear flow characteristics is a challenging design problem due to nonlinearity of valve mechanism and fluidic properties under various operating conditions. In this study, averaging pulse width modulation (PWM) is proposed as a control valve signal by implementing PWM with predetermined duty period so that overflow at the open position and underflow at the closed position are divided proportionately around desired mean flow rates during entire cycle periods. Multichannels in a parallel pattern are implemented to yield linear flow characteristics with higher resolution than a single channel. With pressure and temperature measurements, the volumetric flow rate is determined by an empirical model of flow characteristics across flow control valves at given operating conditions. The experimental results on achieving the desired volumetric flow rate of air under actual flow conditions without a flow meter are presented for viability of the proposed methodology in practical uses.

So, the optimizing control valve signal and the combustion control in this experimental are found by using the trial model. Optimal combustion control of untreated landfill gas is proposed for an effective usage and a low-cost solution in waste to energy technologies. Variations of methane concentration in untreated landfill gas over time cause undesired performance of combustors in thermal efficiency and gas emission. In this work, the experimental investigation on variables of combustion process is systematically presented to determine an inherent performance index of a combustor, reflecting actual thermal efficiency and gas emission for optimal control. Those quantitative findings can be implemented via fuzzy logic rule knowledge based approach to combustion control. From the experimental results of a can-type combustor, it is confirmed that the optimal combustion control of untreated landfill gas yields the desired exhaust gas temperature with maximum thermal efficiency and minimum gas emission under varying methane concentrations or changes of operating conditions. The proposed methodology can be generalized to optimal combustion control of untreated landfill gas via the fuzzy logic rule knowledge based approach, which is the most suitable to characteristics of each combustor.

Keywords: Feasibility analysis, Landfill gas, Power generation, Internal combustion engine, Organic Rankine cycle, Stirling engine, Flow control, Averaging Pulse Width Modulation (PWM), Multi-channel flow, On-off valve, Empirical model, Combustion control, Landfill gas, Low calorific gaseous fuel, Fuzzy logic control.

ACKNOWLEDGEMENTS

I would like to express my deepest gratitude and sincerest appreciation to my advisor Prof. Dr. Thananchai Leephakpreeda, who has provided advisement, expertise, and support throughout the research, along with the use of the Mechanical Engineering Laboratory at the Sirindhorn International Institute of Technology (SIIT), Thammasat University. I have learned so much over the course of my studies and I greatly appreciate the opportunity to work on such an exciting technology, and to have gained the experience that will help me immensely in future endeavors, and in all aspects of life. I would also like to thank all of my peers and mentors in the School of manufacturing system and mechanical engineering (MSME).

Mr. Kanchit Pawananont

TABLE OF CONTENTS

LIST OF TABLES

LIST OF FIGURES

LIST OF SYMBOLS/ABBREVIATIONS

Symbols/Abbreviations	Terms
LFG	LandFill Gas
MSW	Municipal Solid Waste
IEA	International Energy Agency
ICE	Internal Combustion Engine
ORC	Organic Rankine Cycle
STE	Stirling Engine
AF	Air Fuel ratio
AI	Artificial Intelligence
PWM	Pulse Width Modulation
LCOE	Levelized Cost Of Electricity
NPV	Net Present Value
IRR	Internal Rate of Return
PB	Payback Period
CH_4	Methane
CO_2	Carbon dioxide
O_2	Oxygen
CO	Carbon monoxide
N_2	Nitrogen
H_2S	Hydrogen sulfide
H_2	Hydrogen
H_2O	Water vapour
SO_2	Sulfur dioxide
NO_x	Nitrogen oxide

CHAPTER 1
FEASIBILITY ANALYSIS OF POWER GENERATION FROM LANDFILL GAS BY USING INTERNAL COMBUSTION ENGINE, ORGANIC RANKINE CYCLE AND STIRLING ENGINE OF PILOT EXPERIMENTS IN THAILAND

1.1 Introduction and literature review power generation from landfill gas

Solid waste from communities, which is dumped in landfills, has significantly increased every year. It raises a large amount of not only leachate but also annoying odor and inflammable gases within landfill. In fact, landfill gas consists of roughly 50% methane, 40% carbon dioxide, 10% other gases by volume. Therefore, life and environment are harmful when landfill fire takes place. In Thailand, there have been a few technical studies on making use of landfill gas in electricity generation on sites. It was reported that public and private sectors invested to generate electricity from landfill gas where those power plants were launched at Rachathewa, Samut Prakan province with capacity of 1 MW, at Kamphaeng Saen, Nakhon Pathom province with capacity of 870 kW, and at Phanomsarakham, Chachoengsao province with capacity of 2 MW. However, a feasibility study, which accounts for financial assessment, has not been reported in literature for investment. In this study, financial assessment of pilot projects is presented for three potential types of power engines to generate electricity from landfill gas, that is, Internal Combustion Engine (ICE), Organic Rankine Cycle (ORC), and Stirling Engine (STE). Figure 1.1 shows components of the ICE power plant. The landfill gas is directly used as fuel of ICE in producing mechanical power of an electricity generator (J.W. Park et al., 2001; Xuede Qian et al., 2002; Chang-Eon Lee et al., 2002; Roberto Bove et al., 2006; Nickolas J. Themelis et al., 2007; Hamid R. Amini et al., 2013).

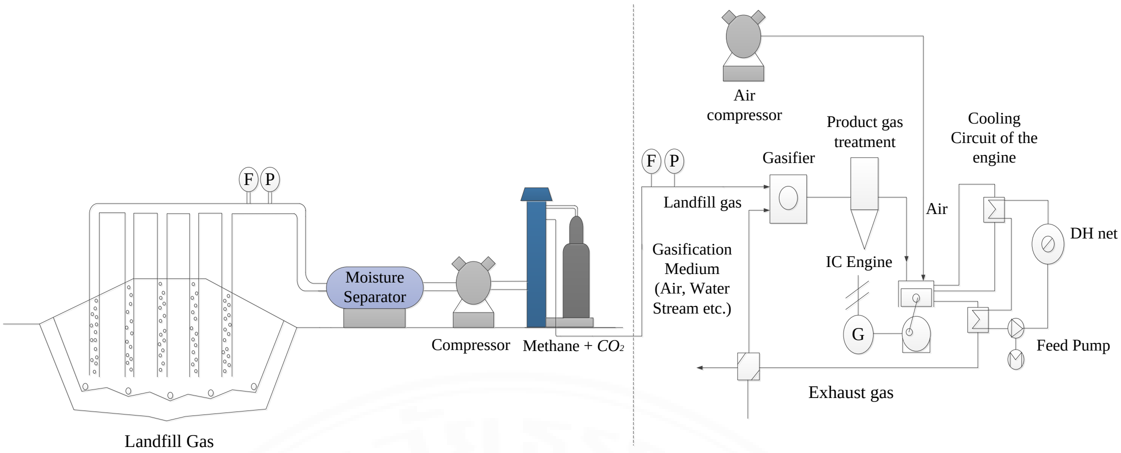

Figure 1.1 ICE power plant by using landfill gas.

In figure 1.2, the components of ORC power plant are a combustion chamber, an evaporator, a condenser, an expander coupled with electricity generator, an air compressor, and organic feed-pump. A refrigerant is evaporated at low temperature by hot air from landfill-gas combustor to drive turbine blades of the expander.

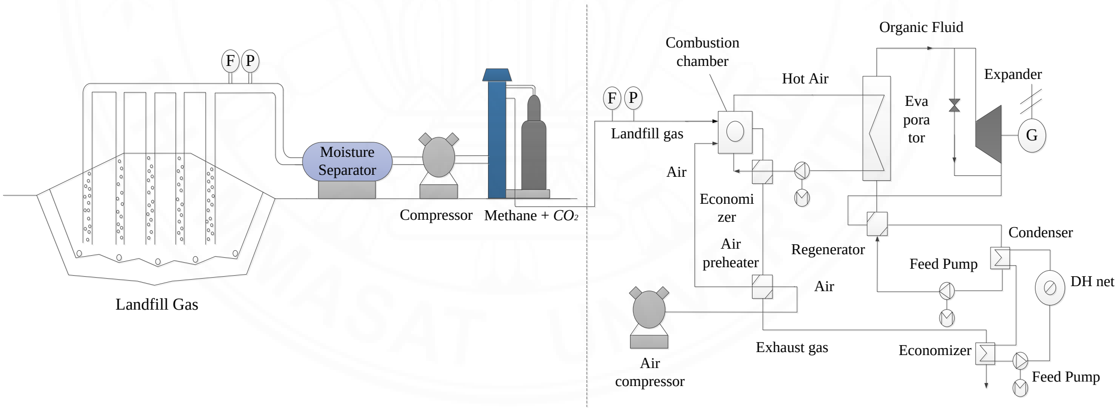

Figure 1.2 ORC power plant by using landfill gas.

For STE power plant, a combustion chamber, Stirling engine, electricity generator, an air compressor, cooling system, and water pump are illustrated in figure 1.3. The landfill gas is burnt out so as to heat up compressed air so as to drive electricity generator.

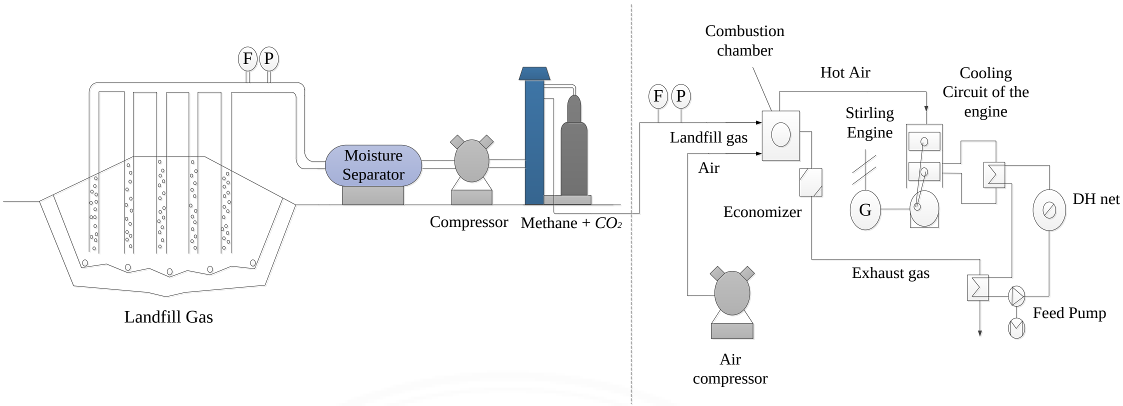

Figure 1.3 STE power plant by using landfill gas.

Although landfill gas is used as fuel in generating electricity, costs of ICE, ORC, and STE power plants are different. Financial indices are to be determined to find the most feasibility in using landfill gas for electricity generation in Thailand. The Levelized Cost Of Electricity (*LCOE*), Net Present Value (*NPV*), Internal Rate of Return (*IRR*), and Payback Period *(PB*) are considered for decision-making process.

1.2 Financial analysis of power plant by using landfill gas

In *LCOE* is commonly used as a financial measure to evaluate electricity production from different methods on a consistent basis. It is regarded as minimum cost per unit of electricity, which is sold to break-even over the lifetime of the project. The *LCOE* is composed of initial investment of installation, construction, and operation/maintenance in each year throughout lifetime. It can be determined by:

$$LCOE = \frac{C_0 + \sum_{t=1}^{n} \frac{M_t}{(1+r)^t}}{\sum_{t=1}^{n} \frac{E_t}{(1+r)^t}} \tag{1.1}$$

where *LCOE* is the cost of electricity per unit of electricity (USD/kWh), C_0 is the initial cost of project (USD), M_t is the cost of operation and maintenance in year t (USD/year), E_t is the electrical power production per year (kWh/year), r is the discount rate (%), and n is the lifetime of the project (year).

The other financial measures are commonly used in feasibility study such as *NPV*, *IRR*, and *PB*. They are written in Eqs. (1.1) - (1.4), respectively.

$$NPV = -C_0 + \sum_{t=1}^{n} \frac{B_t}{(1+r)^t} \tag{1.2}$$

$$-C_0 + \sum_{t=1}^{n} \frac{B_t}{(1+IRR)^t} = 0 \tag{1.3}$$

$$PB = \frac{\text{Cost of the project}}{\text{Average net annual cash inflow}} \tag{1.4}$$

where B_t is the cash flow, which is received in year t (USD / year). The positive *NPV* is preferable for investment while the $IRR \geq$ yield requirements. The *PB* is the basic decision-making criteria when the *PB* should be less than the lifetime of the project.

1.3 Investment analysis of economics

In this section, the financial indices are determined to assess potentials of electricity generation from landfill gas. Technical specifications of pilot projects are set up for this feasibility study. The preparation cost of landfill gas is required to separate unwanted contaminants, such as water, sulfur compounds, ammonia, and carbon dioxide from methane before usage. From technical review, table 1.1 indicates amount of solid waste, costs of installation and maintenance/operation and gas production according to area of landfill. In experimental investigation, it was reported that the power engines ICE, ORC, and STE yields different power outputs from given fuel consumption rates of landfill gas according to capacities as listed in table 1.2

Table 1.1 Technical specification of landfill.

Landfill area	Solid waste	Installation*	Maintenance/operation	Gas production
(rai)	(tons/day)	(million USD)	(million USD /years)	(m^3/h)
65	50	1.11	0.04	180
125	100	1.38	0.06	300

*Excluding land price

Table 1.2 Technical specification of ICE, ORC and STE.

Type	ICE	ORC	STE
Power output	469 kW	150 kW	80 kW
Life expectancy	30 years	20 years	25 years
% Methane	40 – 100%	20 – 100%	18 – 100%
Fuel Consumption	245 m^3/h	120 m^3/h	130 m^3/h

According to table 1.1 and 1.2, various costs, which are listed in table 1.3, are determined under market conditions of Thailand. For example, ICE is widely available while ORC and STE are imported from other countries. In turn, the prices of ORC and STE are higher than ICE. The sizes of the landfill are chosen to match capacity of each power engine. In this study, all the power engines are run for 24-hour electricity generation where this hypothesis might be extreme case to gain the most profit.

Table 1.3 Detailed costs of ICE, ORC, and STE.

Types of cost	ICE 469 kW_e (USD)	ORC 150 kW_e (USD)	STE 80 kW_e (USD)
Power engine	312,584	155,167	71,467
Landfill installation	1,388,889	1,111,112	1,111,112
Gas cleaning systems	116,667	n/a	n/a
Boiler	n/a	13,889	n/a
Exhaust gas	98,195	55,556	55,556
Construction	200,817	41,667	41,667
Maintenance/operation for power engine	21,160	7,322	7,462
Maintenance/operation for landfill	66,667	44,445	44,445

Additionally, table 1.4 provides financial conditions during investment. The life of the projects is considered for twenty years.

Table 1.4 Financial conditions for investment.

Conditions	Description
Engine Depreciation	Efficiency of power engine is reduced at 0.5% per year.
Maintenance cost	3% of total initial cost per year.
Inflation rate	3%
Yield requirements	Interest rate of 7%
Feed-in-tariff	0.15 USD for 10 years and basic inflation rate after 10 years later

From technical and financial conditions above, the values of $LCOE$, NPV, IRR, and PB for each power engine are determined and listed in table 1.5. The power engine ICE yields the lowest $LCOE$ among other power engines since ICE can produce high electricity. It is found that the value of NPV from STE is less than zero. Electricity generation of STE from landfill gas is not advantageous to investment at moment. This result might be caused by the high cost of power engine per unit of power output. All the financial indices are quite satisfactory for electricity generation by using ICE. However, it should be noted that the preliminary interpretation of this feasibility study is based on specified conditions. The implication from numerical results is to be judiciously used.

Table 1.5 Financial indices of each power engine.

Power engine	ICE	ORC	STE
$LCOE$ (USD/kWh)	0.11	0.30	0.42
NPV (USD)	3,739,516	809,215	-566,719
IRR (%)	25.8489544	9.2337856	3.791684
PB (year)	2.82	7.97	21.27

CHAPTER 2
SEQUENTIAL CONTROL OF MULTICHANNEL ON-OFF VALVES FOR LINEAR FLOW CHARACTERISTICS VIA AVERAGING PULSE WIDTH MODULATION WITHOUT FLOW METER : AN APPLICATION FOR PNEUMATIC VALVES

2.1 Introduction and literature review control of on-off valves for linear flow characteristics

Flow control is one of the most critical processes in various industrial applications. In fact, there are different flow control devices, which are often used together with a flow meter and a data acquisition system as shown in figure 2.1(a).

Those mechanical control devices such as valves, variable speed pump, and backpressure regulator are implemented so as to start, stop, regulate, and/or direct the flow of fluid by full or partial operating functions. The variable speed pump supplies flow at variant demand, based on process conditions. The backpressure regulator is used to obstruct the flow by causing a pressure drop across an orifice. Comparatively, flow control valves are much more low-cost and effective in terms of installation, implementation, and maintenance. However, they have their own inherent nonlinear characteristics of passageway for the flow due to the geometrical mechanism of valves and physical properties of fluids. Therefore, flow control is required precisely under such tight constraints. On–off control of the flow control valves is easily accepted among industrial operators due to simple design and straightforward real-time implementation. The flow control valve is either completely open or completely closed. Recently, on–off control methods are acceptably applied to diverse types of valve technology. The high switching frequency in a pneumatic booster was done by a high-speed rotary valve. A novel magnetic valve was developed in lifting off a plug from a valve seat for a wide range of frequencies. An on–off valve was manipulated by a low voltage command in a microfluidic system. A new design of microfluidic on–off valve was attained without an external power source. A high speed on–off valve was coupled with hydraulic propeller in a single module. However, it was not effective for the performance of set-point control where the control for linear flow characteristics is required. There are challenging attempts of researchers in controlling the flow with accuracy. In the position control was implemented by on–off valves with linear open-loop velocity response. However, a small deadband takes place around zero control signals. By using the loop-shaping method, a discontinuous switching model was transformed a linear continuous equivalent model for robust solenoid-valve controlled pneumatic systems. The results of the approach indicated acceptable tracking performance. Alternatively, a sliding mode control law was implemented to on–off valves for pneumatic actuation without using pulse width modulation (PWM), but a chattering motion was observed in experiment. In the attempt, rapid switching on–off valves were used for pressure control of a pneumatic actuator. The flow output had strong nonlinear response to the pressure. In this work, the PWM technique is applied for on–off control of flow. The refined proportional adjustment for desired flow rates is obtained by an averaging PWM implementation for multichannels of flow control valves. Instead of a flow meter, the volumetric flow rate can be determined by empirical models of accessible process variables: pressure and temperature under various operating conditions, as shown in figure 2.1(b), where there is no obstruction to fluid flow. There have been a few challenging attempts of engineering research on flow sensorless control of valves with accuracy and reliability. An artificial neural network was devised as a computation model of the human brain to capture flow characteristics across a proportional pneumatic valve (Leephakpreeda, T. et al., 2003; Xue'en, Y. et al., 2004; Zhu, K. et al., 2012; Hejrati, B. et al., 2013; Mercorelli P. et al., 2014; Werner, N. et al., 2016).

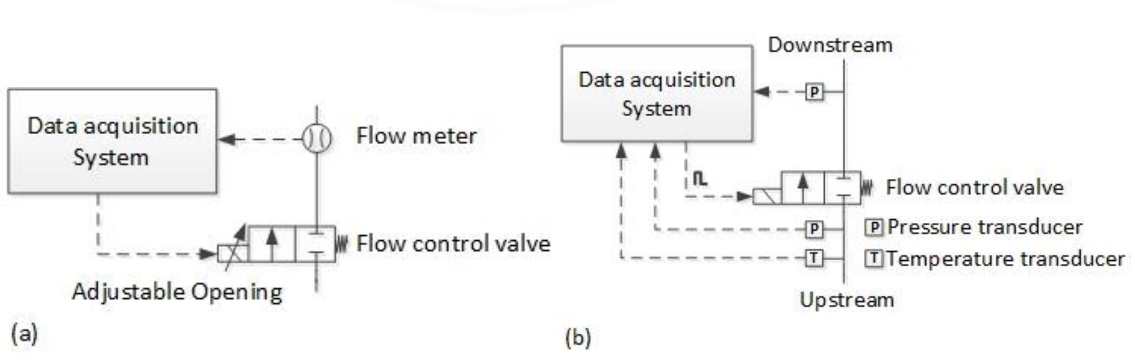

Figure 2.1 Architecture of flow control: (a) conventional type and (b) proposed type.

The feedforward neural network, which was trained with observation data, was implemented to determine flow rate of air as a flow meter. Regardless of time-consuming development, the soft computing method yielded advantage of flow determination where a simple empirical model was not available for the proportional control valve. Conventionally, a state-observer technique was applied to estimate another output such as a speed through measurement of current and voltage for operation of an electromagnetic valve in a variable engine. Similarly, a spool position of a hydraulic valve was accessed by voltage and current of a solenoid valve in a braking system. Besides indirect determination of flow, this approach required rigid quantitative derivation of physical systems. Unlike those inexpensive computing approaches, a piezoelectric module was integrated with hydraulic devices to adaptively control camless engines under compensation of pressure faults. In this paper, the technical contributions are presented as follows. The novel techniques of averaging PWM and multichannel on–off valves are developed analytically and experimentally to confirm the applicability of the proposed methodology for linear flow characteristics with accuracy. The volumetric flow rate is determined for the flow control with an empirical model of flow characteristics across the multichannel on–off control valves at given operating conditions without a flow meter.

The outline of novel contributions in this work is pointed with flow control problems of on–off valves from related works in the most recent state. In the experimental setup is developed to illustrate viability of the proposed sequential control of multichannel on–off valves for linear flow characteristics via averaging pulse width modulation without flow meter in practice. The system flow characteristics of control valves are formulated to understand inherent nonlinearity of flow through control valves, which is caused from flow variables such as temperature and pressure. The technical rationale and descriptions of averaging PWM and multichannel on–off valves without a flow meter are analytically proposed to obtain linear flow characteristics from on–off valves. In experimental results show exemplary applications of the proposed control methodology to airflow through pneumatic valves with accuracy. The conclusive remarks of main findings are given.

2.2 Experimental setup of on-off valves

Figure 2.2 shows a schematic diagram of an experimental rig for determining an empirical model of flow characteristics through the flow control valves and validating effectiveness of the proposed methodology. There are three electrical solenoid valves: SMC™ (Thailand) SYJ512-5 LZ-M5 (NC) with maximum opening frequency of 5 Hz, which are connected in a parallel pattern as the studied module. They are implemented to regulate the volumetric flow of air. The volumetric flow rate of air is detected by the flow meter: FESTO™ (Thailand) SFET3-F500-L-W18-B-K1 of 0–50 L/min with accuracy of 65% full scale. It should be noted that the flow meter is used in a test rig for cross verification whereas the flow control system in this work is proposed without flow meter. Two pressure transducers—FESTO 19563 SDE-1-5V/ 4-20mA of 0–10 bar with accuracy of 60.5% full scale—are used to measure upstream pressure and downstream pressure across the flow control valves. To obtain various operating conditions of airflow, the upstream pressure and downstream pressure are altered by restrictions of two needle valves. In other words, this arrangement simulates variations of pressure sources and fluidic loads across the flow control valves in real processes. The air is compressed under different room temperatures. A type-K thermocouple converter— Shinko™ (General Instrument Co., Ltd., Bangkok, Thailand) DCL-33A-A/M—is installed for temperature measurement of air. A data acquisition system—ARDUINO™ UnoR3-16MHz—reads measurement signals of the pressures, temperature, and flow rate. It is capable of sending command signals to flow control valves in real time.

2.3 System flow characteristics through control valve

Apart from directing flow, valves are commonly used to control amount of fluid flow within piping systems. Technically, the amount of volume flowing though the valve per unit time is

$$\dot{q} = C_V(a)F(P_u, P_d, T) \tag{2.1}$$

where $\dot{q}$ is the volumetric flow rate of the downstream flow across the valve, C_V is the valve coefficient, a is the percentage of opening portion, F is the flow characteristic function, which is strongly dependent upon the upstream pressure P_u, downstream pressure P_d, and upstream temperature of the fluid T.

The volumetric flow rate along with fluid density can be converted to the mass flow rate. Pressure and temperature of compressible fluids are required to determine the density. In this work, the measurements of pressure and temperature are proposed instead of using a volumetric/mass flow meter. Practically, the volumetric flow rate in Eq. (2.1) is regulated by altering open positions of a flow control valve. However, the amount of flow is dependent upon the open positions and the operating conditions of fluid. It can be disrupted when the operating conditions change. The physical properties of the fluid, such as density and viscosity, are defined from operating conditions. For example, an increase in gas temperature causes decreases in density and viscosity.

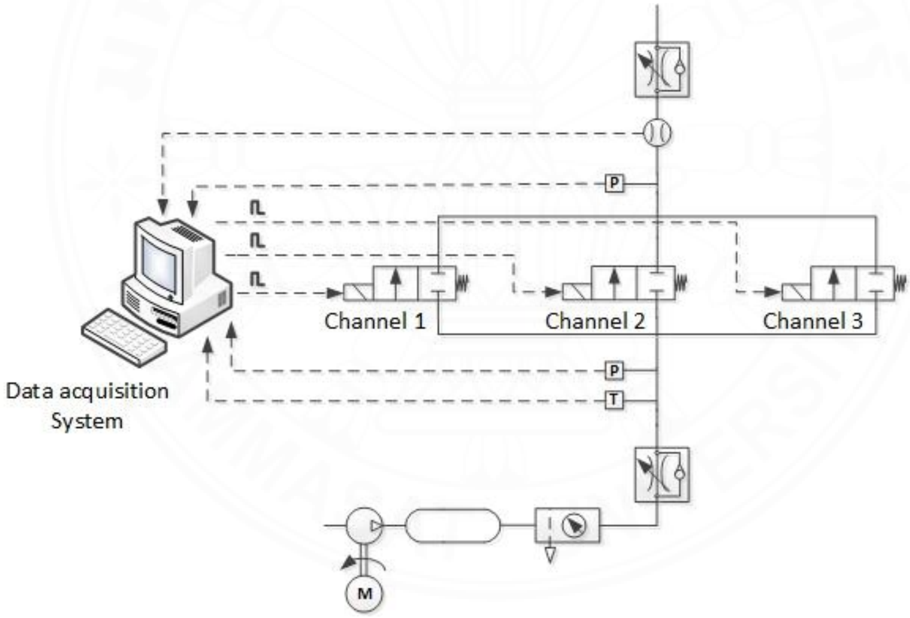

Figure 2.2 Schematic diagram of experimental rig.

Also, changes in the volumetric flow rate come from the upstream pressure and downstream pressure across the flow control valve. In turn, the characteristics of flow through the flow control valve are complicated. To predict flow behaviors, there are various empirical models in capturing those characteristics of flow through the passageway of the flow control valve. In fact, empirical modeling is focused on the relationship of observation data between those flow variables and the volumetric flow rate. For instance, a multilayer feedforward neural network can be applied as a universal nonlinear approximation relating flow variables to the mass flow rate under different operating conditions. The selection of empirical models, available in the literature, can be done in such a way that the predicted values are close to the actual values of the flow. In this paper, the empirical model of a solenoid control valve is proposed for experimental studies of air as

$$\dot{q} = C_d C_o a F(P_u, P_d, T) \tag{2.2}$$

The flow characteristic function is defined as:

$$F(P_u, P_d, T) = \frac{P_u}{\sqrt{T}} \begin{cases} 1 & ; P_{atm}/P_u \le P_r \le P_{cr} \\ C_\gamma \left[P_r^{2/\gamma} - P_r^{(\gamma+1)/\gamma} \right]^{1/2} & ; P_{cr} < P_r \le 1 \end{cases} \tag{2.3}$$

with the pressure ratio P_r, the relevant valve coefficients C_o (kg½K½/J½), C_γ , and the critical pressure ratio P_{cr}

$$P_r = P_d / P_u \tag{2.4}$$

$$C_o = \sqrt{\frac{\gamma}{R\left((\gamma+1)/2\right)^{(\gamma+1)/(\gamma-1)}}} \tag{2.5}$$

$$C_\gamma = \sqrt{\frac{2}{(\gamma-1)} \left(\frac{\gamma+1}{2} \right)^{(\gamma+1)/(\gamma-1)}} \tag{2.6}$$

$$P_{cr} = \left(\frac{2}{\gamma+1} \right)^{\gamma/(\gamma-1)} \tag{2.7}$$

where C_d is the discharge coefficient (L J½/bar kg½min), γ is the specific heat ratio of gas, R is the gas constant (J/kg K), and P_{atm} is the atmospheric pressure (bar). For air, the values of γ and R are 1.4, and 287 J/kg K, respectively.

It should be remarked that Eq. (2.2) is derived from empirical modeling, which is based on experimental observations rather than on physical relations (theoretical modeling). The empirical flow model in Eq. (2.3) is effectively used to predict flow behaviors of air through the solenoid valves from experimental observations. Furthermore, it should be remarked that influences of a pipeline on flow characteristics, such as an inclined pipeline and a noncircular pipeline, are taken into account. In fact, the effects inherently cause changes in flow variables of pressure and temperature at upstream and downstream sides of the flow control valves where the empirical model is derived from those flow variables for the flow characteristics across the flow control valves. Actually, the specific heat ratio γ is usually found in incompressible flow formula.

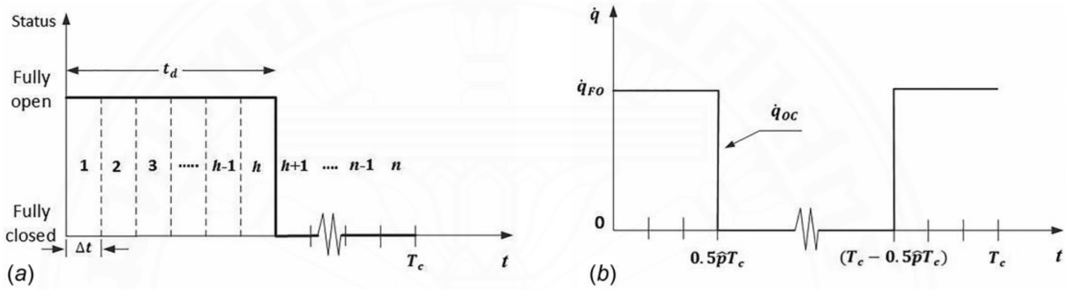

Figure 2.3 Implementation of PWM: (a) conventional type and (b) proposed type.

It involves flow work of gas maintaining a continuous flow due to pressure difference. Dimensional homogeneity is applied for units of flow variables according to measurements in this study. From Eq. (2.2), the volumetric flow rate changes although the flow control valve is regulated at a given opening position. It is significantly dependent upon operating conditions of the upstream pressure, downstream pressure, and upstream temperature as expressed in Eq. (2.3). This nonlinearity of the control valve is very challenging for flow prediction and on–off valve control design.

2.4 Averaging pulse width modulation for flow control

In the proposed architecture, the amount of flow through a pipe is to be regulated by a digital PWM signal in opening or closing the flow control valve, as illustrated in figure 2.1(b). In practice, on–off control valves are designed on the basis that the response time is short in the opening step and the closing step. In analysis, fast response of on–off control valves is valid in generating the volumetric flow rate in such step changes. The volumetric flow rate is estimated by the empirical model of the flow control valve in Eq. (2.1). Knowledge of accessible flow variables, such as the upstream pressure, downstream pressure, and upstream temperature of fluid, is obtained with measurement devices. The flow control valve is open or closed fully in such a way that the required volumetric flow rate is equal to the total amount of volume flowing through the flow control valve per cycle period of a single pulse wave control, T_C. In figure 2.3(a), define the open/closed interval of the flow control valve as Δt. It should be remarked that the open/closed interval can be set to be equal to the sampling time or multiple sampling times of a data acquisition system.

The duty period and the duty cycle of the PWM are, respectively, defined as

$$t_d = h\Delta t \tag{2.8}$$

$$\hat{p} = \frac{h}{n} \tag{2.9}$$

where h is the number of open intervals within a cycle period and $0 \le h \le n$; $n\Delta t = T_C$

According to the definitions, the cycle period T_C is the period of a square PWM wave. The open/closed interval Δt is the elementary time interval that the flow control valve occupies either open position or closed position. The duty period t_d is the time interval that the flow control valve is opened fully within a cycle period. The duty cycle $\hat{p}$ is the percentage of duty period to a cycle period.

The corresponding volumetric flow rate can be represented in terms of a Fourier function as

$$\dot{q}_{OC}(t) = A_0 + \sum_{k=1}^{\infty} A_k \cos\left(\frac{2\pi kt}{T_C}\right) + \sum_{k=1}^{\infty} B_k \sin\left(\frac{2\pi kt}{T_C}\right) \tag{2.10}$$

with

$$A_0 = \frac{1}{2T_C}\int_{-T_C}^{T_C} \dot{q}_{OC}(t)dt \tag{2.11}$$

$$A_k = \frac{1}{2T_C}\int_{-T_C}^{T_C} \dot{q}_{OC}(t) \cos\left(\frac{2\pi kt}{T_C}\right) dt \tag{2.12}$$

$$B_k = \frac{1}{2T_C}\int_{-T_C}^{T_C} \dot{q}_{OC}(t)\, sin\left(\frac{2\pi kt}{T_C}\right) dt \tag{2.13}$$

where $\dot{q}_{OC}$ is the amount of flow during full opening or closing of the flow control valve, and is the time.

In the proposed methodology, the volumetric flow rate is regulated by flow control valves as a square function with a cycle period. In particular, it can decompose a periodic square function into the sum of harmonics. Therefore, the analysis is valid since a Fourier series is a periodic function in terms of an infinite sum of sines and cosines. The volumetric flow rate through the flow control valve in Eq. (2.10) is equal to the actual volumetric flow rate, as the flow control valve is fully open while it is zero as the flow control valve is fully closed. It can be seen in Eq. (2.1) that the flow rate at a given time is dependent upon the open/closed positions of the flow control valve and the pressure of fluid across the flow control valve. Those characteristics of flow restriction are complicated in regulating the flow rate according to the desired level, even though the linear opening of the flow control valve exists.

The averaging PWM technique is proposed for accuracy of flow control, as illustrated in figure 2.3(b).

By integrating Eqs. (2.11)–(2.13) with amplitudes of $\dot{q}_{FO}$ (fully open) and zeros (fully closed) during the cycle period, the results are given by

$$A_0 = \hat{p}\dot{q}_{FO} \tag{2.14}$$

$$A_k = \frac{\dot{q}_{FO}}{k\pi}\left(sin(k\pi\hat{p}) - sin\big(2k\pi(1-0.5\hat{p})\big)\right) \tag{2.15}$$

$$B_k = 0 \tag{2.16}$$

Like conventional PWM signals, the averaging PWM signals can be generated in practice by multiplying sinusoidal signals up to

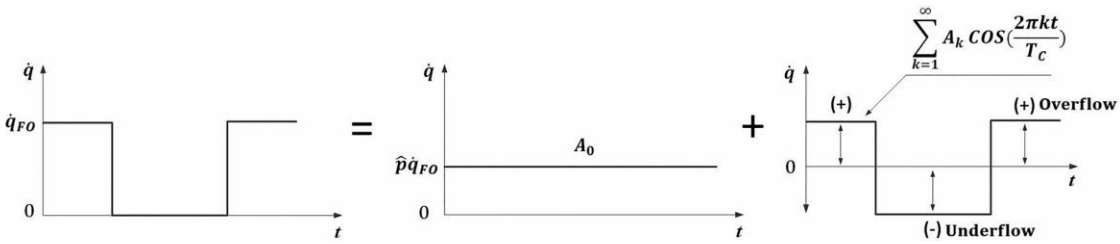

Figure 2.4 Interpretation of averaging PWM.

the threshold harmonics for each sampling period. The value of $\dot{q}_{FO}$ is the volumetric flow rate where the flow control valve is fully open or a = 100% in Eq. (2.1), for a given operating condition. From figure 2.4, it can be interpreted from Eqs. (2.14)–(2.16) that the volumetric flow rate is regulated with the flow control valve by adding more volumetric flow rate to the mean value of the volumetric flow rate of $\hat{p}\dot{q}_{FO}$ during the duty period and removing more volumetric flow rate from the mean value of the volumetric flow rate of $\hat{p}\dot{q}_{FO}$ during the remaining time of T_C .

Eventually, the required volumetric flow rate is obtained by the mean value at a given cycle period. Unlike the conventional PWM, the averaging PWM is defined where the duty period is broken into two equal durations. They are specified at the starting interval and ending interval of the cycle period. This arrangement yields overflow during the former half of the duty period and the latter half of the duty period after underflow. In turn, the overflow does not take a long time in one time within a single cycle period. The actual volumetric flow rate is able to closely track the required volumetric flow rate through a cycle period. To see the advantages of the averaging PWM signal over conventional PWM signal, an exemplary simulation, as shown in figures 2.5(a) and 2.5(b), demonstrates the performances of PWM signals with a magnitude of 1 and a cycle period of 1 s in regulating an output variable of a first-order process. From an open-loop response, it can be observed that the output variable, which is regulated by the averaging PWM signal, follows closely around the output variable, which is regulated by an analog signal with magnitude of 0.75. The plots of tracking differences and mean tracking differences are illustrated in figures 2.5(c) and 2.5(d), respectively. In this case, the mean tracking difference is determined to be -0.002 at final time. On the other hand, the conventional PWM signals results in the cases of overflow with mean tracking difference of 0.024 and underflow with mean tracking difference of -0.021 to the output variable during transient. Mathematically, the averaging PWM is fundamentally same as a conventional PWM with a phase shift. The effects of control action seem to be identical, but they are different with a shifted response when the flow control process is steady. In fact, a steady flow process rarely takes place in control applications. On the other hand, actual flow processes are continuously unsteady if flow control valves are required. In those dynamic cases, the averaging PWM is performed to ensure minimization of overflow and underflow at each cycle period when the flow control valves take actions. Therefore, the averaging PWMs are important to be implemented on every single cycle period for satisfaction of flow control all the time.

It can be seen that the duty cycle of the on–off flow control valve is determined from the required volumetric flow rate by

$$p = \frac{u}{\dot{q}_{FO}} \tag{2.17}$$

where *u* is the required volumetric flow rate.

Without loss of generality, the value of u is less than or equal to the value of $\dot{q}_{FO}$, which is greater than zero. This assumption means that the usable volumetric flow rate is available in flow control. If it is not valid, then the value of *p* is set to be unity at

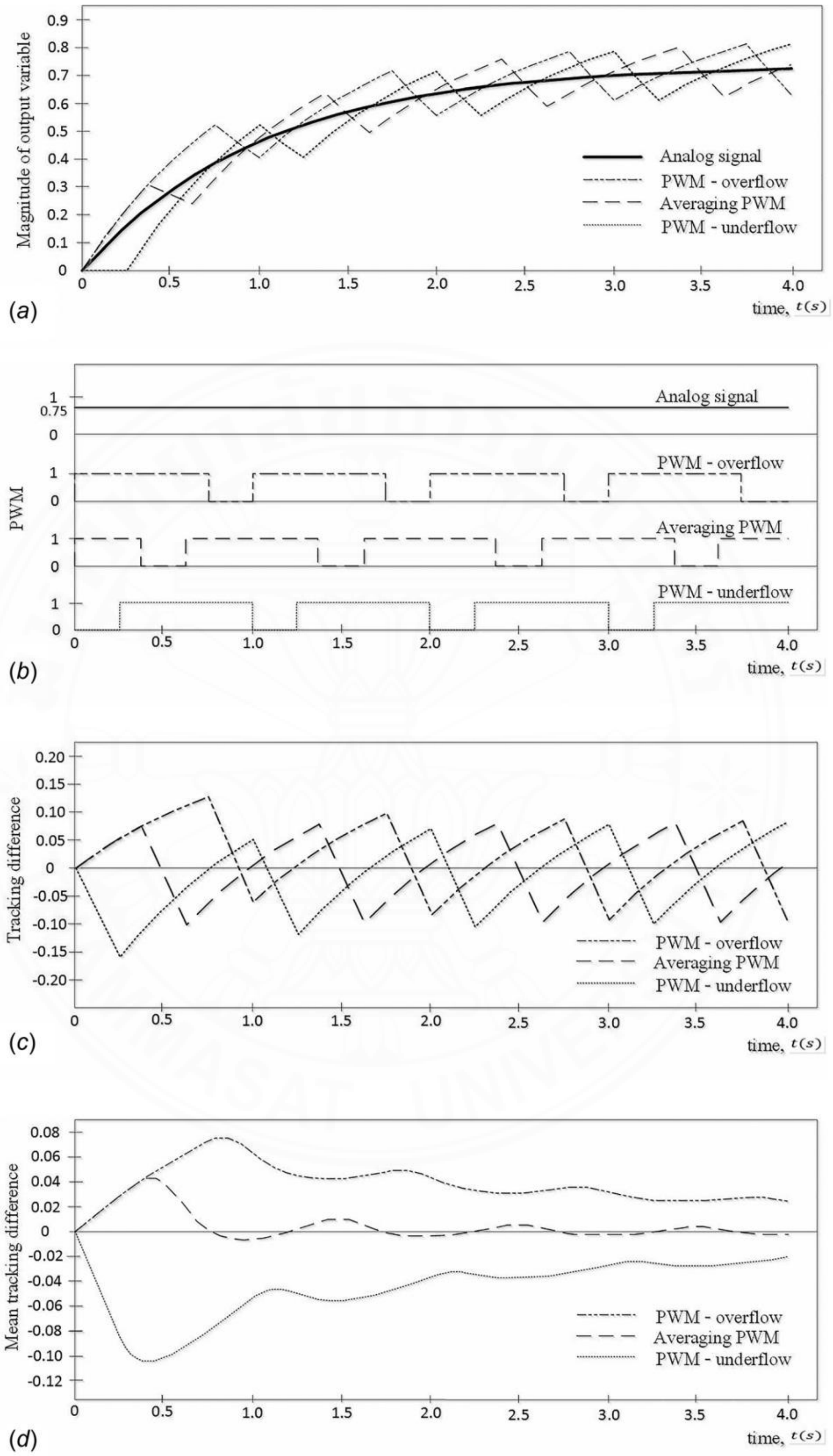

Figure 2.5 Comparisons of averaging PWM compared with conventional PWM: (a) open-loop responses, (b) PWM inputs, (c) tracking differences, and (d) mean tracking differences.

full opening of the flow control valves. The value of *p* is used to manipulate the flow control valve to accurately open within the duty period. In turn, the required volumetric flow rate is obtained successfully in flow processes. This demand can be accomplished completely when the ratio of the number of open intervals within a cycle period to the total number of open/closed intervals in Eq. (2.9) approaches the ratio of the required volumetric flow rate to the volumetric flow rate at full opening of the flow control valve

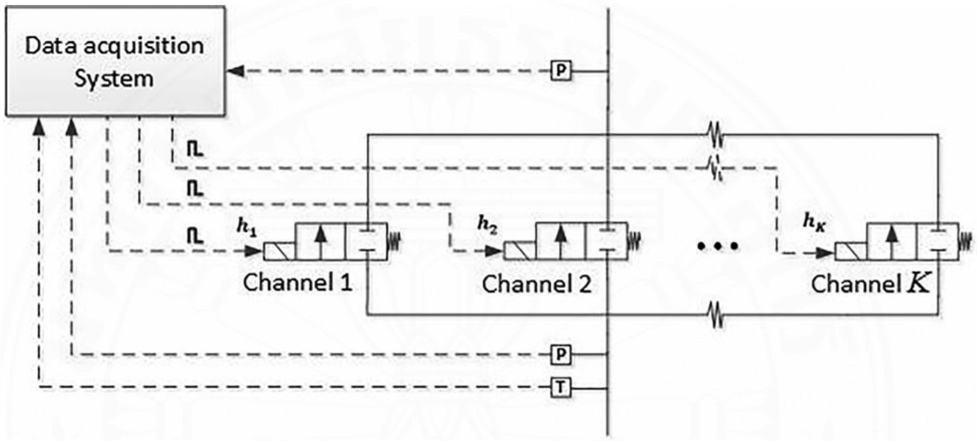

Figure 2.6 Module of multichannel flow control valves.

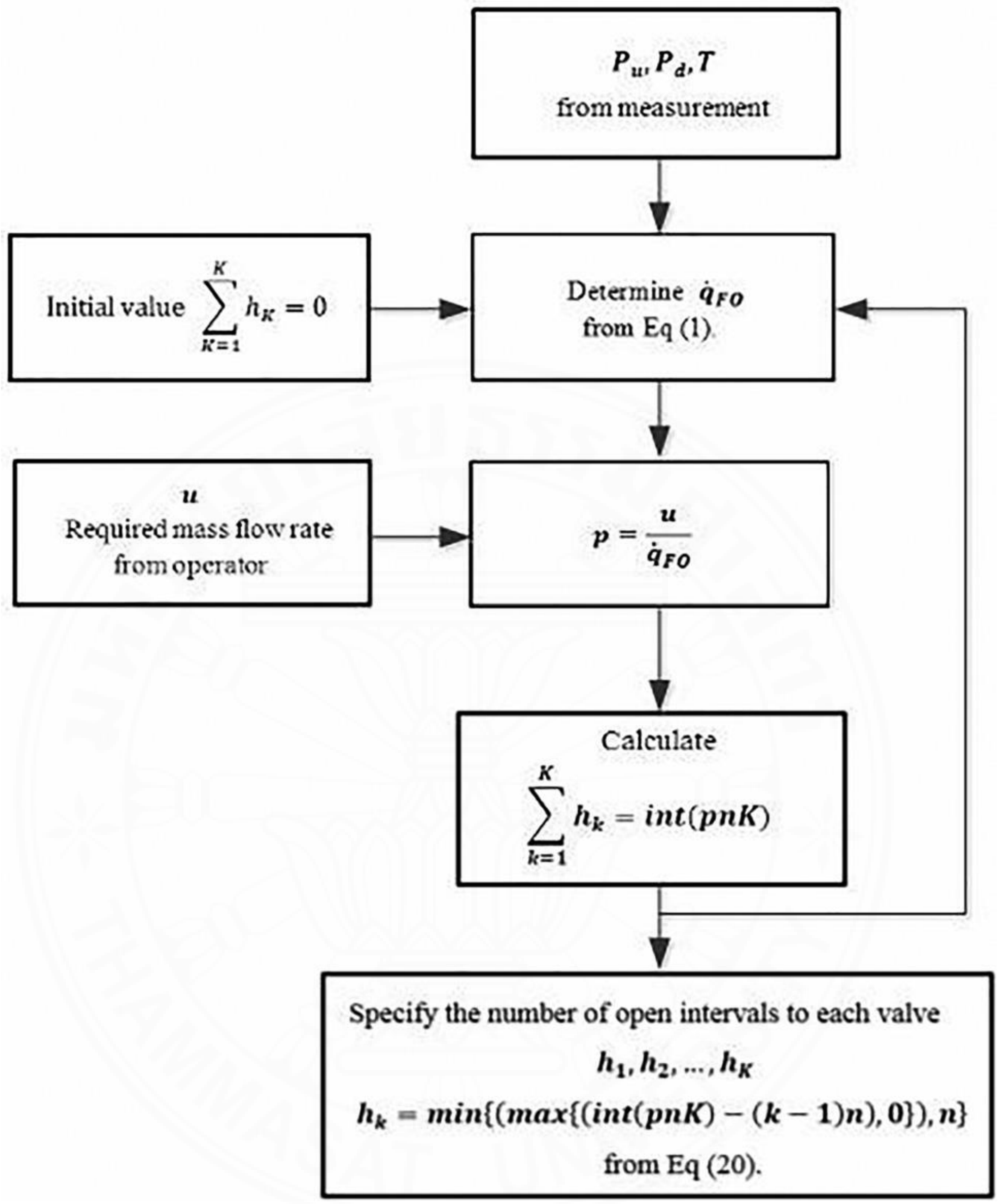

Figure 2.7 Determination of number of open intervals to multichannel flow control valves.

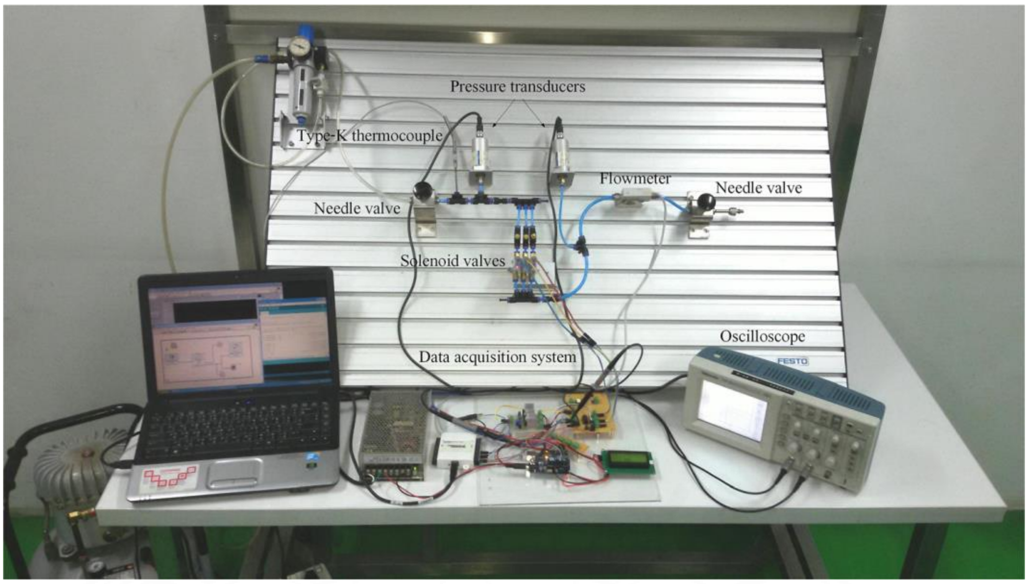

Figure 2.8 Experimental setup of flow control valves.

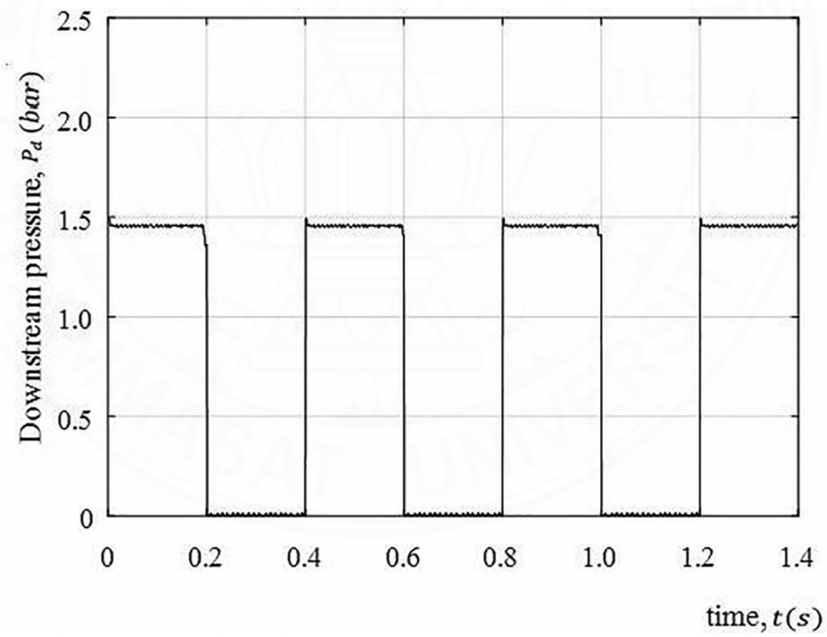

Figure 2.9 Experimental observation of closing/opening valve from downstream pressure.

in Eq. (2.17), or $\left(\hat{p} = \frac{h}{n}\right) \rightarrow p$. Technique by using multichannels of the flow control valves is proposed to obtain higher resolution than a single channel in conventional practice. For analysis on the effects of overflow and underflow based on figure 2.5, a performance index *I* is defined as the absolute mean value of integral of time multiplied by error, as expressed in the below equation:

$$I = \frac{1}{T_C^2}\left|\int_0^{T_C} (T_c - t)e(t)dt\right| \tag{2.18}$$

where *e* is the error between the full flow rate $\dot{q}_{FO}$ or zero and the required volumetric flow rate *u*.

The errors occurring early in a cycle period result in undesired responses for long time within a cycle period. It weights errors which exist after start of the cycle period much more heavily than those at end of the cycle period. The absolute value is used for considering the real value without regard to the sign from resultant outcome of overflow or underflow. For the best performance, the value of *I* is zero. It is true when the full flow rate $\dot{q}_{FO}$ or the nonflow rate is required at the cycle period. For other required volumetric flow rates, the performance index I_A in the case of the averaging PWM figure 2.3(b) and I_C in the case of the conventional PWM figure 2.3(a) are determined to be zero and $0.5p(1-p)q_{FO}$, respectively. It can be seen that $0 = I_A < I_C$.

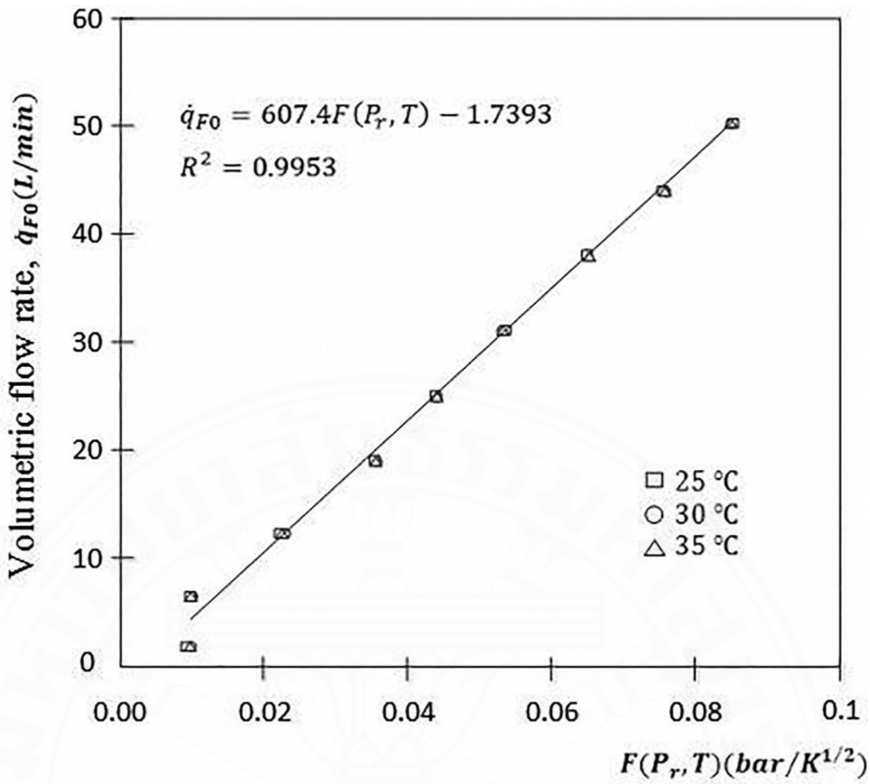

Figure 2.10 Linear regression analysis of empirical model for three channels.

Compared to the conventional PWM, the balanced flow control of the averaging PWM yields less deviation of the process output close to the desired volumetric flow rate as it is implemented during the cycle period.

2.5 Multichannels of the Flow Control Valve for Fine Flow Control

As mentioned earlier, accuracy in controlling the volumetric flow rate can be obtained when the duty cycle $\hat{p}$ (integer ratio)

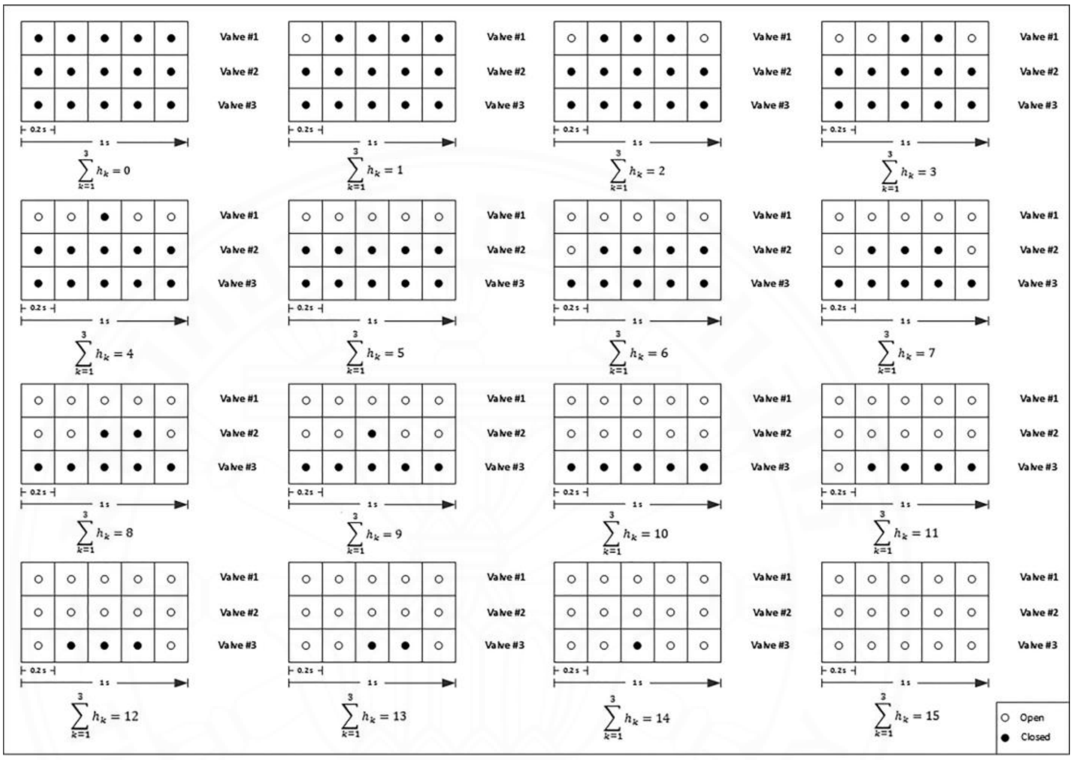

Figure 2.11 Status of three solenoid valves for different values of $\sum_{k=1}^{3} h_k$.

approaches any real numbers of *p*. The improvement of adjusting the volumetric flow rate can be done by increasing the total number of open/closed intervals within the cycle period. In other words, this method must reduce the open/closed intervals as small as possible. However, this adjustment is limited by the response time of the flow control valves in opening/closing operations due to mechanical inertia. In this work, the total number of the open/closed intervals is increased by increasing the numbers of channels of the flow control valves as illustrated in figure. 2.6

The flow control valves are assembled in a parallel pattern. In real-time implementation, all the flow control valves are fully closed for zero volumetric flow rates. They are open and closed according to the number of open intervals within the cycle period when the volumetric flow rate needs to increase. All the flow control valves are fully open when the maximum volumetric flow rate is needed. To implement this proposed technique, the value of $\hat{p}$ in Eq. (2.9) is replaced by

$$\hat{p} = \frac{\sum_{k=1}^{K} h_k}{nK} \tag{2.19}$$

where K is the total number of channels. To determine the total number of the open intervals according to the required volumetric flow rate, the duty cycle of the on–off flow control valves in Eq. (2.17) is applied to Eq. (2.19) as

$$\sum_{k=1}^{K} h_k = \text{int}(pnK) \tag{2.20}$$

where ( ) is the nearest integer function.

This result yields the assignment of the number of open intervals for each flow control valve in the below equation:

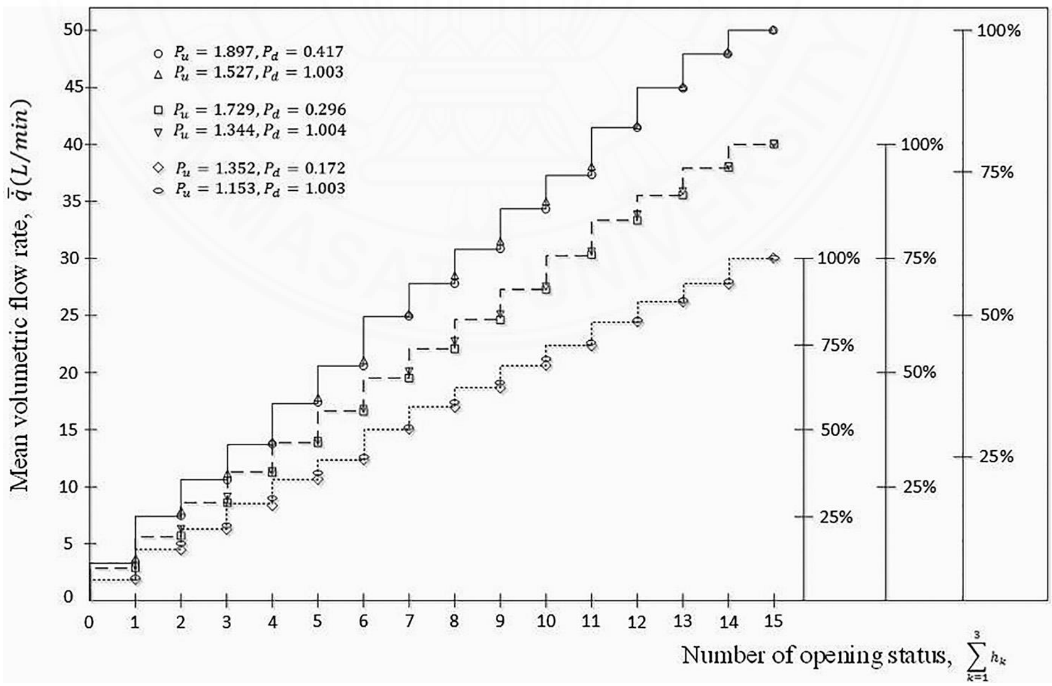

Figure 2.12 Performances of flow control of three channels under operating conditions.

$$h_k = \min\{(\max\{(\text{int}(pnK) - (k-1)n), 0\}), n\} \quad (2.21)$$

With Eq. (2.21), total number of open intervals of the K-valve module ($\text{int}(pnK)$) is divided into the number of open intervals h_k for each channel, $k = 1,...,K$. An example of calculation according to Eq. (2.21) is demonstrated in the Appendix. It can be noticed in Eq. (2.19) that the number of open intervals within the cycle period is increased to the sum of the open/closed intervals from the total channels of the flow control valves (nK) In other words, the value of $\hat{p}$ approaching the value of *p* is closer than a single channel. The value in Eq. (2.20) is estimated to command the opening of the flow control valves so as to yield the required volumetric flow rate $u = p\dot{q}_{FO}$ under given operating conditions. The value of *p* is determined from Eq. (2.17) when the value of $\dot{q}_{FO}$ is calculated from the empirical model in Eq. (2.1), which is substituted with measured variables of pressure and temperature. The real-time implementation of the proposed methodology, as shown in figure. 2.7.

2.6 Results and discussion for control on – off valves

Figure 2.8 depicts the experimental rig of airflow control as described in figure 2.2. Three solenoid valves are subjectively installed in a parallel pattern such a way that the volumetric flow rate can be adjusted proportionally with open/closed interval of 0.2 s.

As seen in figure 2.9, a delay in valve operation is not found by observing square signals of downstream pressure during opening and closing of valves in experiment. In fact, positions of closing and opening cannot be detected directly. However, it is expected that the entire square signals of closing/opening positions take place because of excluding rising time of pressure transducer. Therefore, the response times of valves are negligible. To determine the volumetric flow rate through the flow control valves, the empirical model of the flow characteristics in Eq. (2.2) is derived from observation data. The pressures across the flow control valves and the temperature of air are varied over operating conditions at full open positions of the flow control valves. The upstream pressure, downstream pressure, upstream temperature, and volumetric flow rate of air are measured for modeling. In realtime implementation, the flow control valves are embedded with knowledge of the flow characteristics in the form of the empirical model without a flow meter. Also, the volumetric flow rate at full open positions cannot be obtained from measurement of a flow meter when the averaging PWM is implemented in control as described in figure 2.7. Correspondingly, the variables of $F (P_r ; T)$ are calculated from Eq. (2.3) with measured data of the upstream pressure, downstream pressure, and upstream temperature of air. Figure 2.10 shows plots of the volumetric flow rate against $F (P_r ; T)$ within a full measurement range of the flow meter.

Linear regression analysis is applied, and the empirical model at full open positions of the three solenoid valves is obtained as

$$\dot{q}_{FO} = 607.4F(P_r, T) - 1.7393 \tag{2.22}$$

The overall valve coefficients in Eq. (2.2) can be determined from the slope of Eq. (2.22) where a = 100%. The coefficient of determination R^2 is 0.9953, which indicates very good agreement

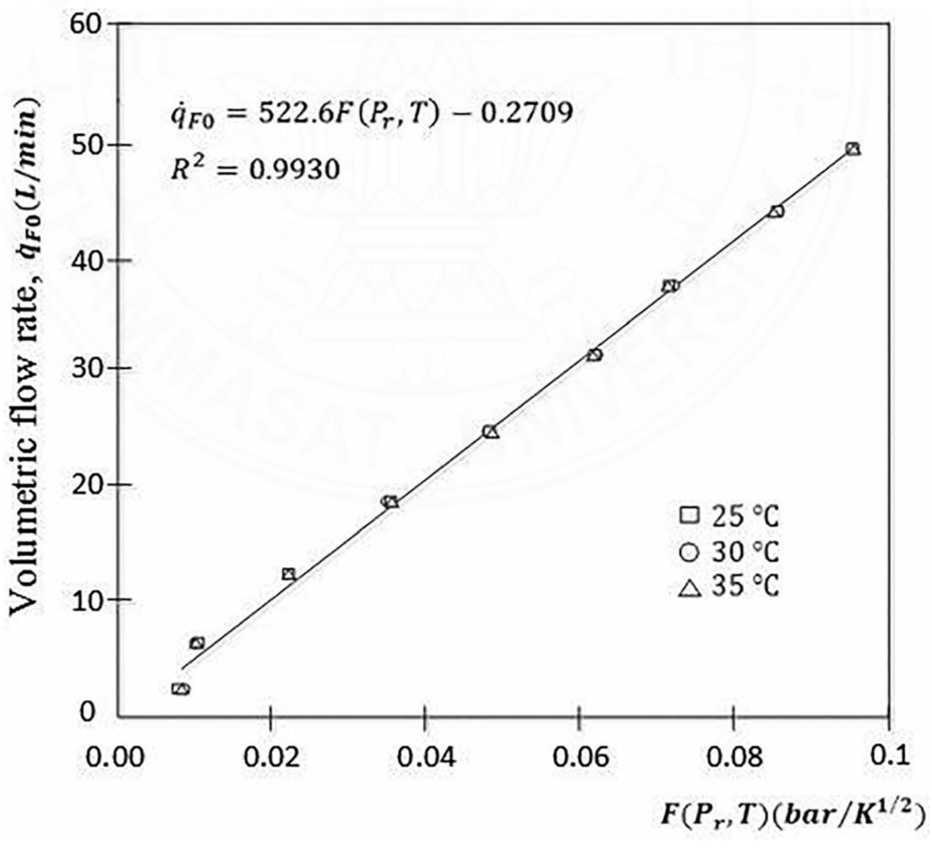

Figure 2.13 Linear regression analysis of empirical model for a single channel.

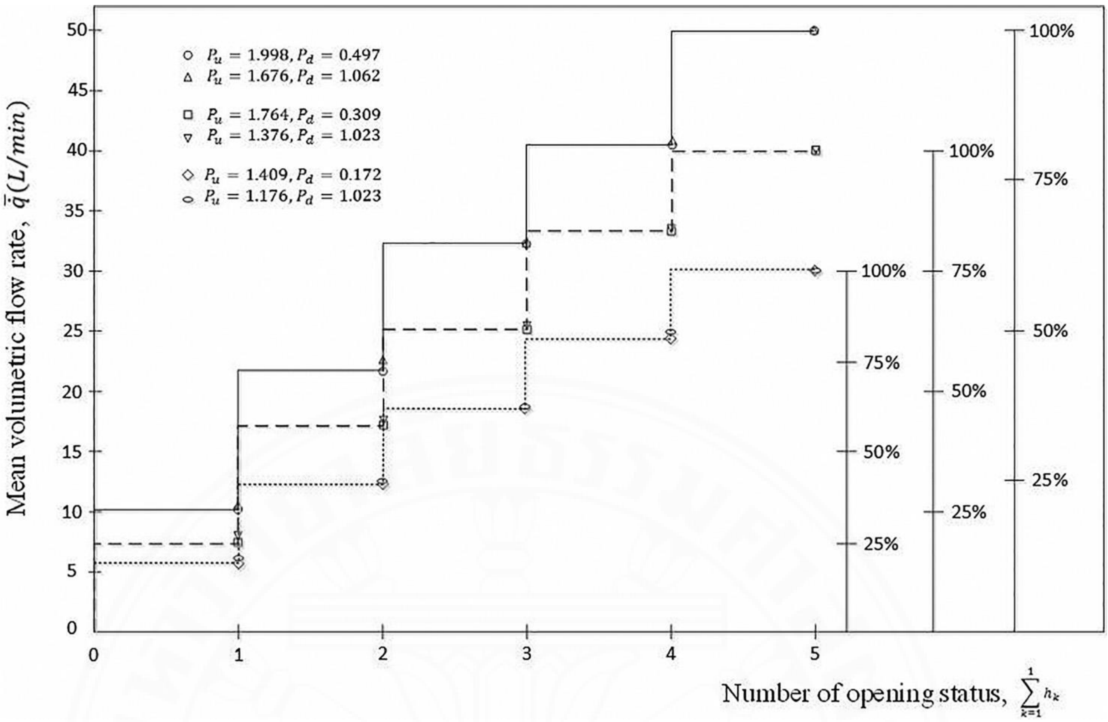

Figure 2.14 Performances of flow control of a single channel under operating conditions.

between measured values and calculated values of the volumetric flow rate for given *F(P$_r$; T)*. The volumetric flow rate at full open positions in Eq. (2.17) can be determined from Eq. (2.22) at given operating conditions. It should be noted that Eq (2.22) is derived when the three solenoid valves open fully. When one solenoid valve opens and two solenoid valves open, Eq. (2.22) can be applied to determine $\dot{q}_{FO}$ by multiplying factors of 3/1 and 3/2, respectively. This multiplication is required since the full volumetric flow rates of those two cases are regulated at 1/3 and 2/3 of $\dot{q}_{FO}$ of three flow control valves. In particular, when a single flow control valve out of three valves is operated, Eq. (2.22) yields 1/3 of the full flow rate. Similarly, when the second flow control valve is operated, Eq. (2.22) yields 2/3 of the full flow rate. In the experiment, the three solenoid valves have a maximum opening frequency of 5 Hz. Therefore, the smallest value of the open/closed interval, Δt, is set to be 0.2 s. There are three channels for improvement of accuracy, that is K = 3. Suppose that (n = 5) is subjectively chosen in this study. The total numbers of open/closed intervals within the cycle period are n = 5, and the cycle period is equal to $n\Delta t$ = 1 s. In fact, the total numbers of the open/closed intervals are to be maximized for accuracy while the cycle period is minimized for fast responses of the flow control valves. Unlike a single channel, multichannels can be applied for 15 (*nK*) cases, including a case of the full closing, within a cycle period, as illustrated in figure 2.11. Figure 2.12 illustrates the performance of sequential control of multichannel on–off valves for linear flow characteristics by using three channels. It can be observed that the flow control valves supply the airflow proportionally under different operating conditions where the upstream pressures and downstream pressures are indicated at full opening positions. The mean volumetric flow rate within a cycle period increases while the number of open intervals increases.

To see better performances than a single channel, the same consideration of empirical modeling can be done by setting $K = 1$. Similarly, figures. 2.13 and 2.14 show the empirical model and the flow control for a single channel. Although the cycle period is 1 s, the volumetric flow rate at full open position is discretized more widely than three channels. This means that the flow control valve with a single channel can respond for supplying air within 1 s; however, the volumetric flow rate may not exactly match the required volumetric flow rate as it is compared with three channels. It should be noticed that the full flow rates through the three valve module and the one-valve module are the same at 50 L/min. Therefore, the slope of 607.4 L $K^{1/2}$/bar min in figure 2.10 and the slope of 522.6 L $K^{1/2}$/bar min in figure 2.13 are close each other. The slight difference of slopes is caused by different structures of modules.

Figure 2.15 illustrates the dynamics of the mean volumetric flow rate through the flow control valves when different reference values (dashed line) are needed from initial time to 10 s. It can be observed that the volumetric flow rate is properly regulated in proportion to the required volumetric flow rate. Specially, the flow control valves can perform step responses according to the set points without any settling time. At a time of 19 s, the downstream pressure is changed by a sharp upsurge while the flow control valves are capable of remaining at the required volumetric flow rate at the desired value of 17 L/min afterward by adjusting the number of open intervals.

As illustrated in figure 2.16, the performances of one-valve module, two-valve module, three-valve module, and four-valve module without a flow meter are further investigated under ramp references where the root-mean-square errors (RMSEs) are determined to be 2.8844 L/min, 1.4606 L/min, 1.0212 L/min, and 0.9627 L/min, respectively. For a single valve with flow meter, the RMSE under the same ramp references is determined to be 3.4346 L/min. It can be observed that the RMSE of the four-valve module without a flow meter is one of the least values among the other modules. Analytically, it indicates that the four-valve module is capable of regulating actual flow rate closest to the desired flow rate since it can achieve linear flow characteristics with the highest resolution. To be compared with a conventional PWM control, the single valve with a flow meter is performed to regulate the flow rate based on corrective actions. It is found that the one-valve module without flow meter can regulate the volumetric flow rate with less RMSE than a single valve with a flow meter. As a result, the proposed averaging PWM implementation enhances the one-value module to regulate the mean flow rate with higher accuracy than the conventional PWM.

However, a selection of the number of valves is concerned for a cost-effective system. In this work, figure 2.17 illustrates numerical comparison of cost and performance of valves among the cases.

It is found that the trend in accuracy extensively increases (decreasing RMSEs) when the multichannel valves are implemented. On the other hand, the cost of valves increases proportionally according to the number of valves. Apparently, there is a tradeoff between controlling flow accurately and reducing cost of valves.

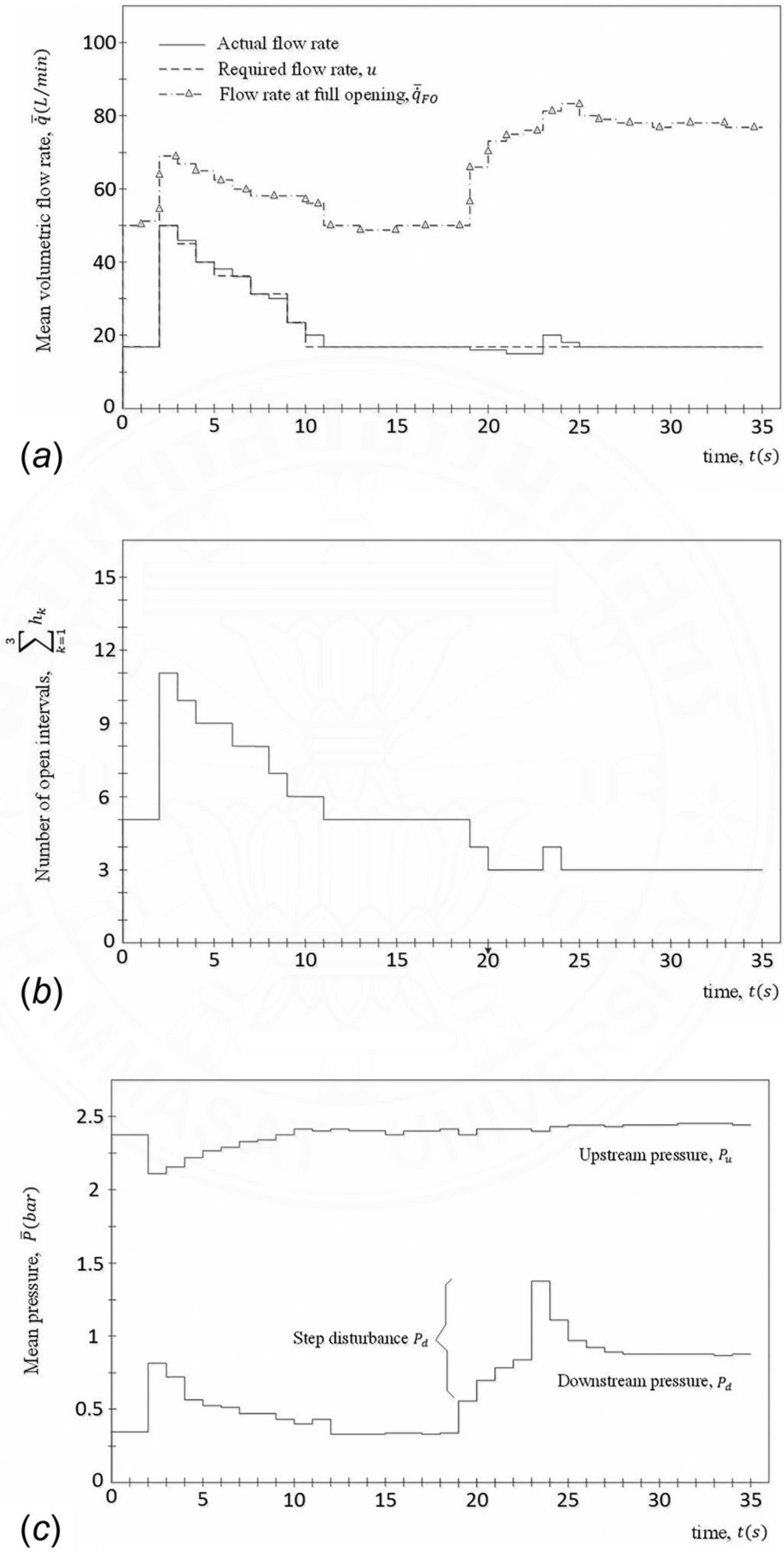

Figure 2.15 Sequential control of three channel flow control valves according to demand: (a) volumetric flow rate, (b) number of open intervals, and (c) pressure.

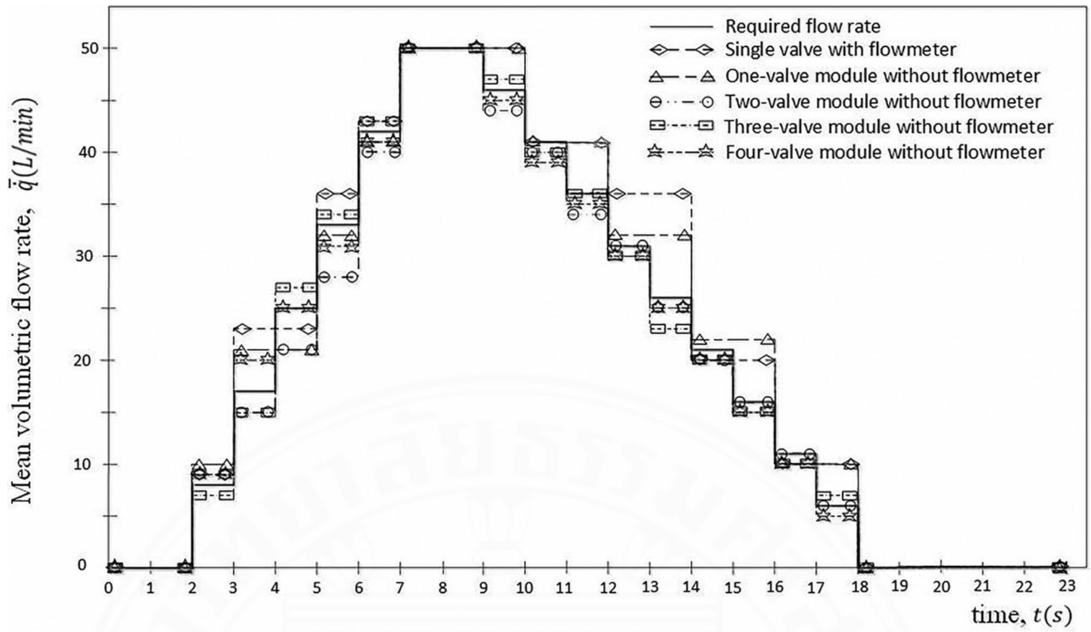

Figure 2.16 Comparison on performances of proposed valves and single on–off valve with flow meter.

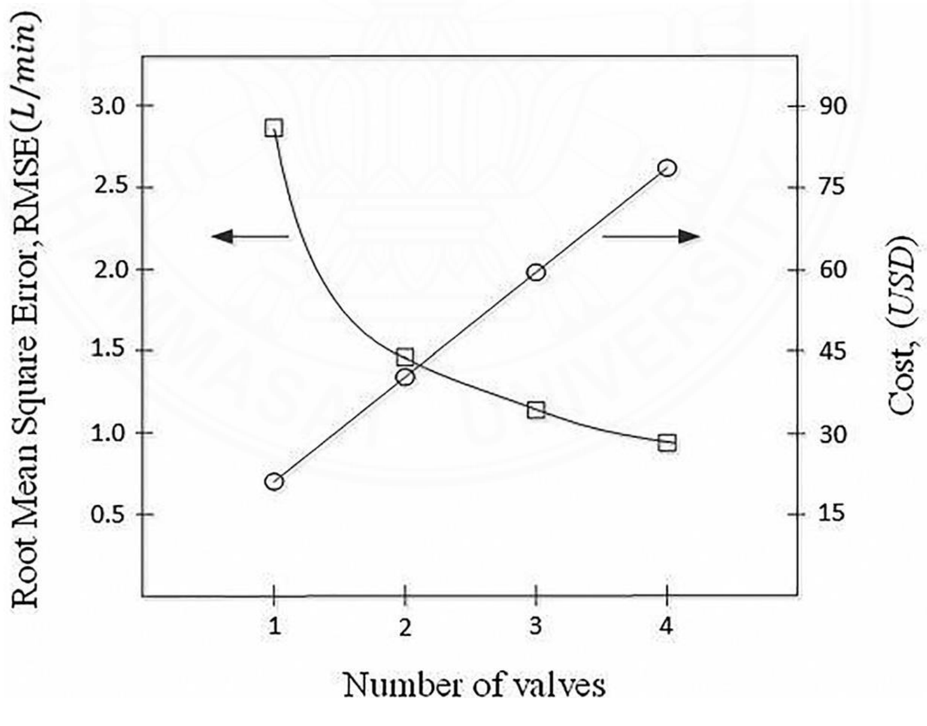

Figure 2.17 Tradeoff between cost and accuracy for selecting number of valves.

A decision making deemed to be optimal is recommended on a case by case basis where low-cost on–off valves have already been accessible in industrial markets.

CHAPTER 3
EXPERIMENTAL INVESTIGATION AND OPTIMAL COMBUSTION CONTROL OF UNTREATED LANDFILL GAS VIA FUZZY LOGIC RULE KNOWLEDGE BASED APPROACH

3.1 Introduction and literature review optimal combustion control via fuzzy logic rule

Recently, the research studies about direct utilization of untreated landfill gas in combustion processes have been demanding as a low-cost solution in waste to energy technologies, for resolving waste managing problem and energy demand. The landfill gas is a high potential energy source as a promising alternative for a fossil fuel to an internal combustion engine, an organic Rankine system, and a Stirling engine in electrical power generation with acceptable financial feasibility. Also, it was reported that the methane dual fuel concept successfully counteracted high nitric oxide and particulate matter emission in a conventional diesel engine. However, the untreated landfill gas is not suitable as a low calorific gaseous fuel with low methane content for feeding engines since it is mitigated with inert carbon dioxide. Actually, it can be enriched to improve thermal efficiency. For example, the mean of accelerated carbonation of bottom ash can been implemented at a laboratory scale with decreasing carbon dioxide concentration by 10% of volume. Apparently, there are significant costs and highly required energy input to enrichment process even though engines produce electricity with negative carbon dioxide emission. Additionally, soot and gas emissions from a direct injection methane gas engine was found to cause environmental impacts. Therefore, the combustion of untreated landfill gas is increasingly needed to be investigated for best practice. Under open filed conditions, the landfill gas is produced with variations of concentrations in methane and carbon dioxide over time. Besides, a predetermined treatment with or without irrigation during the process can alter amount of organic matter and biological activity for methane production. It is challenging in combustion control of the untreated landfill gas that thermal requirements of combustion, such as exhaust temperature for heat exchange, is specified at the desired points, and the exhaust emission to environment is minimized, as the concentrations of methane and carbon dioxide vary over time during combustion processes. Up to now, there has not been any research on experimental investigation and control of the untreated landfill gas in combustion processes. The technical limitations, which are resolved by control in this study, have drawn combustion of untreated landfill gas away from practical usages. For example, in the variability of methane content in landfill gas causes instability of burning operation and narrow operating range. Control of valves for linear flow characteristics is difficult due to properties of landfill gas under various operating conditions. The combustion characteristics of landfill gas are known at early state of research study about influencing factors of combustion stability. Increasing carbon dioxide content reduced laminar burning velocity. The variations of methane/carbon dioxide concentrations in landfill gas make combustion control difficult for both analysis and real time implementation (P.Braga e Rita C.O. Sebastião et al., 2013; Jeffrey W. Martin et al., 2013; Francesco Di Maria et al., 2014; Sudarshan Kumar et al., 2015; Wei Chen et al., 2016; Kyung Chun Kim et al., 2017; Haisheng Zhen et al., 2018).

Therefore, the development of optimal combustion control technique for untreated landfill gas is worthy of investigation in literature. In this study, the effects of the methane concentration, carbon dioxide concentration, and percentage of excess air on thermal efficiency and exhaust emission are experimentally investigated from combustion of the untreated landfill gas. With knowledge of those interactions, the control strategy is proposed by adjusting the flow rates of the untreated landfill gas and supply air so that thermal efficiency is maximized but gas emission is minimized in real time implementation. The fuzzy logic rules based approach is applied to determine the linguistically controlling laws for robustly optimal combustion of the untreated landfill gas under variation of methane concentration where the advantage is that the solution is understandable for control design and implementation (Wei Li et al., 2000; Soteris A. Kalogirou et al., 2003; Jean-Pierre Corriou et al., 2008; Leephakpreeda, T. et al., 2011; Pitikhate Sooraksa et al., 2012; Nuchkrua, T et al. 2013; Zhangfeng Qin et al., 2014; Anna Vasičkaninová et al., 2015; Nuchkrua, T et al., 2016; Chun-Fei Hsu et al., 2016).

3.2 Experimental setup of combustion system

As illustrated in figure 3.1, the untreated landfill gas, within a storage tank, is prepared for experiments with the gases mixed from two gas tanks of pure methane and carbon dioxide. A carbon dioxide sensor of Sprintir^{TM} is mounted on the storage tank to gauge the concentration of carbon dioxide with a measuring range of 0-100% by volume and accuracy of ± 1% while the methane concentration is calculated from the remaining concentration accordingly. The concentrations of methane and carbon dioxide in the untreated landfill gas are adjusted by proportionally opening two flow control valves. The air for combustion control is pumped into a supply tank. A premix chamber is used to generate and ignite the mixture of the untreated landfill gas and supply air according to commanded proportions. A can-type combustor of 25.4 mm diameter and 730 mm length is designed to yield combustion of the untreated landfill gas. The normal flow of the untreated landfill gas and the normal airflow are supplied to the premix chamber for maintaining stability in combustion process. Like the supply air, the volume flow rate of the untreated landfill gas is regulated from altering the controlled flow with a proportional flow control valve, which is successfully developed, before the untreated landfill gas enters the premix chamber. Two fuzzy logic controllers regulate the volume flow rates of the untreated landfill gas and supply air at desired points via two normally closed flow control valves of Hana^{TM} H2001-12VDC. The temperature of exhaust gas and the concentration of oxygen are measured as the inputs of the fuzzy logic controllers, compared with the reference points of temperature and oxygen concentration. The automatic control and measurement are handled in real-time implementation by a data acquisition system of NI MyRIO^{TM}-1900. For the experimental investigation in finding the optimal operating conditions, the *CO* and *NOx* emissions in exhaust gas are manually measured by Testo^{TM} 350. A k-type thermocouple with a measuring range of 293-1250 ºC and accuracy of ±0.75% / ºC is installed at the exit of the combustor where the oxygen sensor of Ninsen^{TM} is installed to measure the concentration of oxygen in a range of 0-25% of volume and accuracy of ±0.5 %. The measurement devices are installed in front of thermal load in practice.

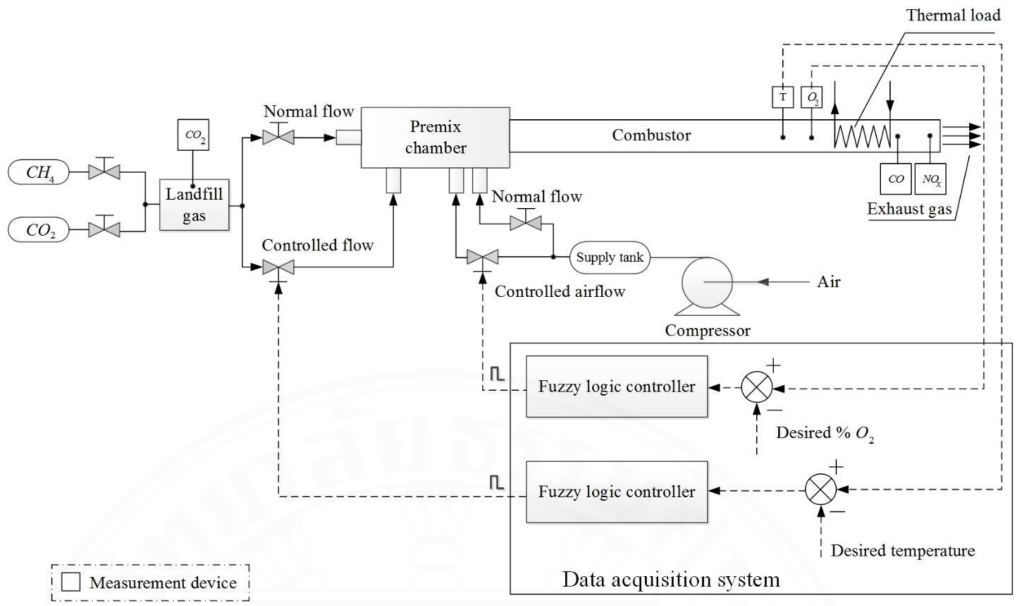

Figure 3.1 Experimental rig for combustion control of untreated landfill gas.

3.3 Untreated landfill gas through combustion processes

Landfill gas is a compound of different gases that is naturally produced by anaerobic reaction of microorganisms from a landfill over time. As shown in figure 3.2, the disposal of waste materials is covered with the layers of soil and woodchips within a waste cell in a liner system.

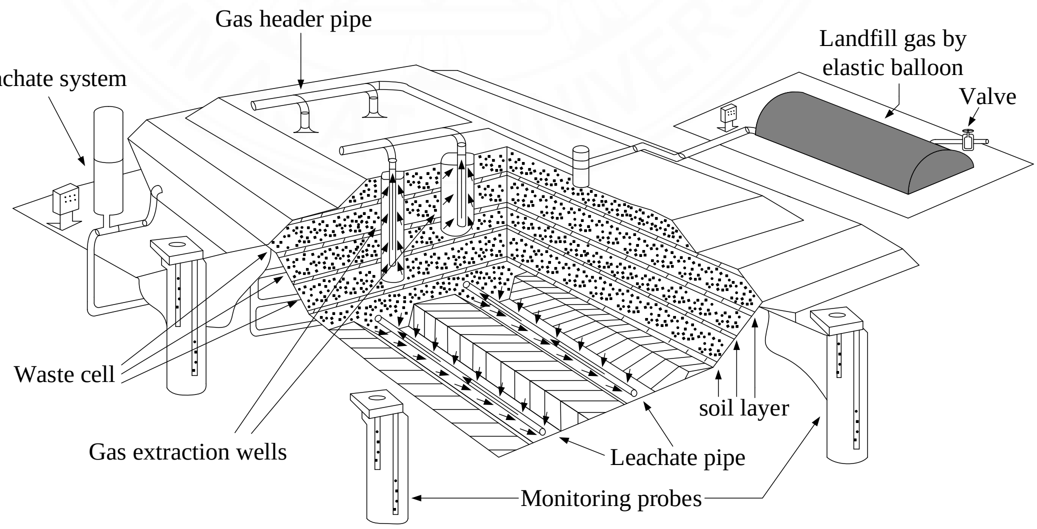

Figure 3.2 Gas production within landfill.

There are six main stages of conversion from solid waste to landfill gas, such as waste organic fraction, aerobic degradation, hydrolysis/fermentation, acetogenesis, methanogenesis, and oxidation. The landfill gas is pumped from gas extraction wells through gas header pipes according to monitoring probes. Also, leachate under the landfill is recirculated so as to percolate all over the place of landfill as a leavening agent. The landfill gas is stored in a gas container for usage. Those processes undergo until the waste materials are used up. In table 3.1, the landfill gas consists of methane, carbon dioxide, nitrogen, oxygen, hydrogen, water vapor, and other volatile organic compounds. During methanogenesis state, methane for burning in combustion is particularly generated as a major portion of the landfill gas. However, the amount of methane is varied with a wide range of percentage by volume of 45%-60% where it is dependent on several factors such as age of landfill, size of lanfill, season, and types of wastes. For example, figure 3.3 shows variation of landfill gas at different stages over time under laboratory conditions. It can be observed that the landfill gas contains methane, carbon dioxide, and other miniature gases with various amounts in time. Furthermore, the concentrations of those gases changes much drastically under open field conditions.

Table 3.1 Composition of landfill gas.

Compound	Average concentration (% by volume)
Methane (CH_4)	45 - 60
Carbon dioxide (CO_2)	40 - 60
Nitrogen (N_2)	2 - 5
Oxygen (O_2)	0.1 - 1.0
Hydrogen (H_2)	0 - 0.2
Water vapour (H_2O)	Saturated
Other	0 - 1.0

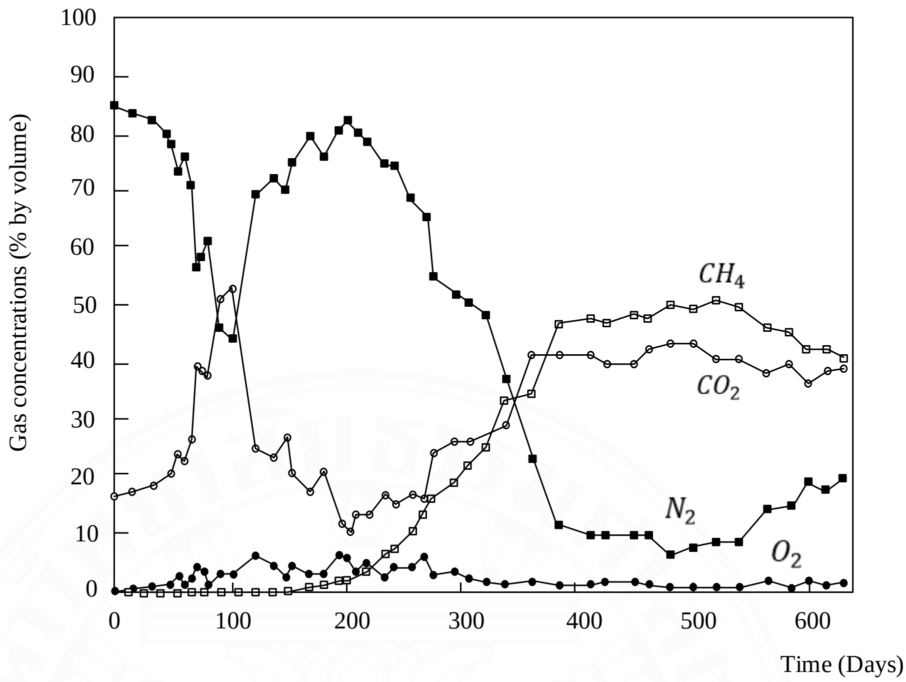

Figure 3.3 Evolution of landfill gas in time under laboratory conditions.

Therefore, direct usage of landfill gas or the untreated landfill gas in combustion is not feasible to maintain heating capacities at desired levels since amount of methane varies according to operating conditions of landfill well. Additionally, emission gases may be developed in different portions. Up to now, the combustion characteristics of landfill gas have not been known for efficient usages of landfill gas. To understand this phenomenon, pure methane, which is burned with oxygen, is described for a base in this study whereas the landfill gas (methane and carbon dioxide), which is burned with air (oxygen and nitrogen) is experimentally studied to be controlled for effective burning. There are three reactions in combustion of methane.

$$CH_4 + 2O_2 \rightarrow CO_2 + 2H_2O \tag{3.1}$$

$$2CH_4 + 3O_2 \rightarrow 2CO + 4H_2O \tag{3.2}$$

$$2CO + O_2 \rightarrow 2CO_2 \tag{3.3}$$

From Eqs. (3.1 - 3.3), each reaction is activated according to operating factors such as amounts of oxygen, combustion temperature, and characteristics of combustion chamber. It can be seen that the emission outcomes are carbon dioxide, and carbon monoxide, including water. Also, the amounts of heat are released with difference, accordingly. However, combustion of landfill gas is complicated since main components are methane and carbon dioxide while air mainly consists of nitrogen and oxygen. Therefore, carbon dioxide and nitrogen cause more incomplete combustion reactions of methane reacting with oxygen. Eq. (3.4) presents the generalized description of combustion of the untreated landfill gas.

$$aCH_4 + bCO_2 + c(O_2 + 3.76N_2) \rightarrow dCH_4 + fCO_2 + gH_2O + hO_2 + kH_2 + mCO + nNO_x \tag{3.4}$$

where a , b , c , d , f , g , h , k , m , and n are the unknown moles, depending on process conditions. The inherent characteristics of combustors are defined in mixing the supply air and the landfill gas and burning the landfill gas for heat. Preferably, excess air is supplied to complete the combustion process. However, the hazardous CO and NO_x emissions from combustion of untreated landfill gas can be found under various operating conditions. In this experimental study, it is observed that the CO gas drastically remains in the exhaust gas after the combustion of the landfill gas has less amount of supply air. On the other hand, excessive amount of supply air to the combustion causes much NO_x gas. To reduce those negative effects, amounts of untreated landfill gas and air are efficiently controlled in combustion process so as to obtain desired heating capacity and acceptable emission. As shown in figure 3.1, the schematic diagram of combustion control of untreated landfill gas is proposed as a multiple-input multiple-output closed-loop control system. It can be seen that the control actuation involves adjusting two flow rates of the untreated landfill gas and supply air. According to Eq. (3.4), the first term and the second term of the reaction equation are quantified in combustion processes where these control outputs are altered over time. Consequently, the heat output and exhaust emission can be manipulated. For a given content of methane, untreated landfill gas is burnt with suitable amount of supply air for efficient combustion. Increasing the flow rate of untreated landfill gas is expected to gain elevated heat output, vice versa. Accordingly, adjusting the supply air is tightly required to obtain low gas emission. Moreover, the methane concentration of untreated landfill gas is not fixed in time. This uncertainty make the optimal combustion control of untreated landfill gas challenging. The flow rate of untreated landfill gas is expected to be altered due to variations of methane content so that the heat output is maintained at the desired level. Experimental investigation of untreated landfill gas combustion is proposed to develop the relevant fuzzy logic rule knowledge for the control.

3.4 Fuzzy logic rule knowledge based approach for combustion control

In this work, a fuzzy logic control system is developed to ensure the best practice for the problem of adjusting the flow rates of the untreated landfill gas and the supply air through a combustor, as the combustion is understood. In control structure, the reference point for the exhaust temperature is defined from the requirement of thermal load where the untreated gas is supplied to be burned to obtain the desired exhaust temperature. In addition, the air is to be supplied to the premix chamber so as to reach obtainable maximum temperature of exhaust air for a given amount of untreated landfill gas, as well as minimum concentrations of carbon monoxide and nitrogen oxide. The supply air is required to be adjusted properly, as well. It is found in experiments that temperature of exhaust gas, carbon monoxide concentration, and nitrogen oxide concentration are functions of oxygen concentration in the exhaust gas. This mathematical relation is proposed as:

$$PI = f(T_e(p), c_{co}(p), c_{NOx}(p)) \tag{3.5}$$

where PI is the performance index of combustion, p is the oxygen concentration in exhaust air, T_e is the exhaust air temperature, c_{co} is the carbon monoxide concentration, and c_{NOx} is the nitrogen oxide concentration. In Eq. (3.5), the oxygen concentration in exhaust gas at optimal point is determined from the maximum value of performance index, which maximizes temperature of exhaust gas at desired temperature for a given flow rate and methane concentration of the untreated landfill gas and minimizes carbon monoxide concentration, and nitrogen oxide concentration, at the same time. The oxygen concentration in exhaust gas is adjusted at the optimal value as the reference point by regulating the supply air in the combustion control. For example, the flow rate of supply air to combustion is increased as the oxygen in exhaust gas is highly left from combustion, and vice versa. The flow control valves of the untreated landfill gas and the supply air are open or closed in such a way that the temperature of exhaust gas and the percentage of oxygen concentration are regulated at the desired outputs of combustor for the thermal processing process with low emission gases. A pulse width modulation (PWM) control technique is to provide intermediate mean amount of the required flow rate from opening and closing the on/off flow control valves for a given duty period. Actually, the duty period of the PWM control is equal to the sampling time in a data acquisition system. Figure 3.4 shows the characteristics of an on/off switch of the flow control valve via PWM signals. The PWM parameters are defined by the duty period of the PWM control signal t_u, and the percentage of open period u where 0%≤ u ≤100%. For example, if u = 0%, then the flow rate through the control valve is null while if u = 100%, then the flow rate through the control valve is full. The partial flow rate is obtained with the u percentage of open period.

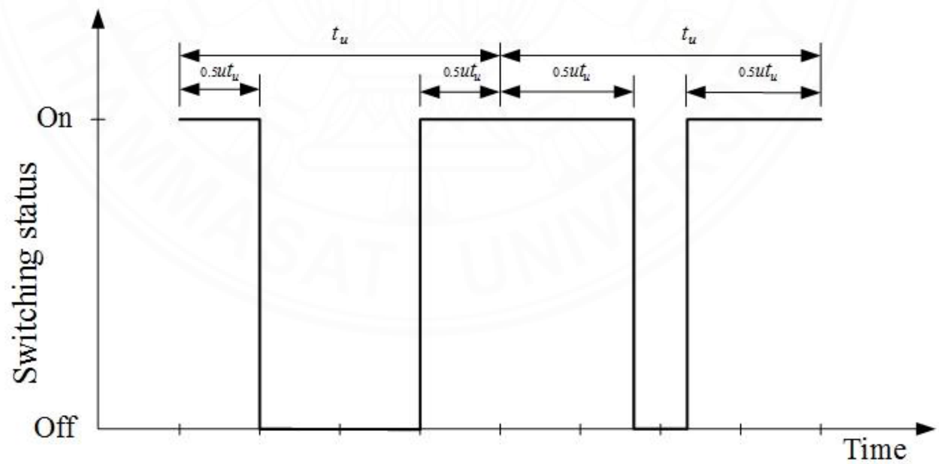

Figure 3.4 PWM generator for switching flow control valves in duty period.

The analytical findings of combustion are used to provide a description of how to control the combustor for a thermal processing system in the linguistic control strategy without precise quantitative knowledge/mathematical models. Intuitively, the temperature of exhaust gas increases or decreases when the untreated landfill gas is supplied more or less than the normal flow, respectively, by using the controlled flow. Similarly, the amount of supply air can be adjusted from the normal airflow to change amount of emission gases. The typical architecture for implementing a fuzzy logic control is depicted, as illustrated in figure 3.5

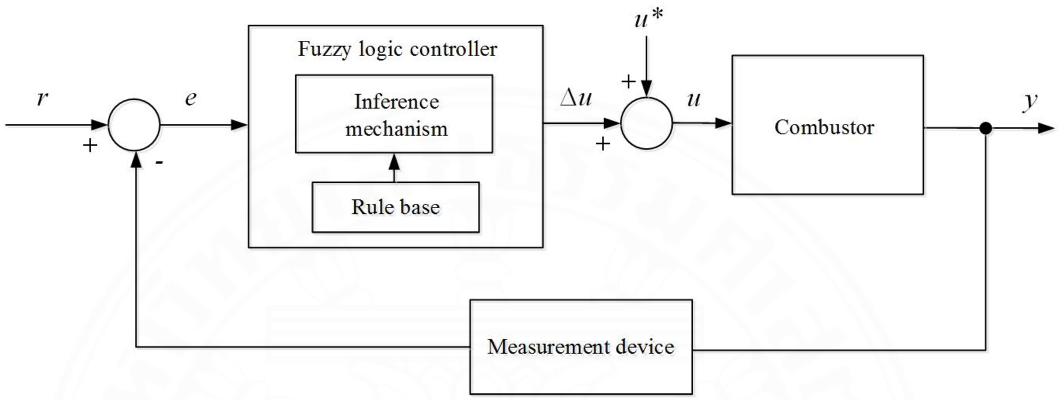

Figure 3.5 Schematic diagram of fuzzy logic control in regulating untreated landfill gas through combustor.

The Δu denotes the controller output, that is the increasing percentage of open period from the normal percentage of open period, u^*, where the performance of the combustor is driven from opening/closing the flow control valves according to the percentage of open period, ($u = u^* + \Delta u$), in a duty period to supply the controlled flows of the untreated landfill gas and supply air through the combustor. The y denotes the measured output of the combustor, such as the temperature of exhaust gas or the oxygen concentration in exhaust gas, while the r denotes the desired output, such as the desired temperature of exhaust gas or the optimal point of the oxygen concentration in exhaust gas from Eq. (3.5). The goal is to regulate the controller output through the combustor such a way that the measured output is maintained at the desired output or the error e is minimized. The fuzzy logic controller is developed to implement error e between the desired output and the measured output to make control decision. Without loss of generality, analytical expression of N -rule base is formed for proportional control laws at any given instance at the two adjacent rules j and $j + 1$ with inherent stability robustness as follows.

R_j: If e is A_j than Δu is B_j .

R_{j+1}: If e is A_{j+1} than Δu is B_{j+1} .

where (A_j , B_j) and (A_{j+1}, B_{j+1}) are the fuzzy subsets of the errors and the fuzzy logic controller outputs at rules j and j + 1, respectively. Typically, they might be referred in control laws as linguistic terms, such as positive, negative, and zero. For example, a control action rule is formed as "if e is negative then Δu is positive." Figure 5.3 shows definitions of fuzzy sets in universe of discourse, as their membership functions are defined between null to unity. By the compositional rules of inference, the fuzzy controller output or the increasing percentage of open period is determined as:

$$\Delta u = \left[1 - S_j(e - E_j)\right] U_j + \left[1 - S_j(E_{j+1} - e)\right] U_{j+1} \qquad (3.6)$$

where E_j and E_{j+1} are the two adjacent points, which e lies on that interval, S_j is the slope of the membership function in the rule j, U_j and U_{j+1} are the controller outputs at the centroid of area if the j^{th} rule or $j + 1^{th}$ rule is the only applicable rule, respectively. The analytical description of the fuzzy logic control law in Eq. (3.6) can be formulated to deal with dynamic behaviors of the combustor. Those parameters of the fuzzy logic controller must be tuned for a given combustor. Some guidelines with an experienced recommendation are provided in results and discussion. In this work, a class of the rule-based knowledge for the proportional-type controller output is defined as follows. If the error is A_j, then the increasing percentage of open period is B_j . The control rules are implemented in real-time implementation according to the error. Correspondingly, Eq. (3.6) are determined to obtain the increasing percentage of open period for opening or closing during a duty period of flow control valves. In turn, the flow rates of landfill gas are regulated so that the error approaches to zero. In the same consideration, the fuzzy logic controller for supply air can be implemented simultaneously, as illustrated in figure 3.1.

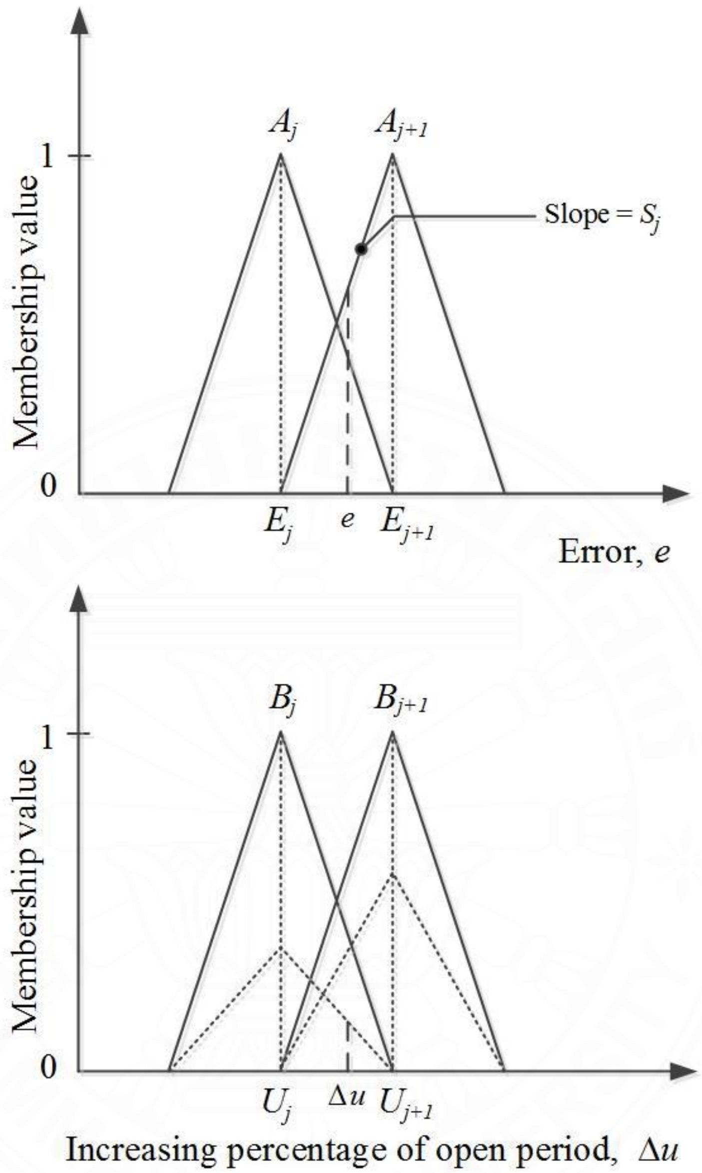

Figure 3.6 Membership functions of fuzzy sets under composition rules of inference.

3.5 Results and discussion optimal control design of combustion

The combustion performance of a test rig using a can-type combustor, as shown in figure 3.7, is investigated to obtain a performance index for best practice, where the temperature of exhaust gas is maximized at the desired level for a given flow rate and methane concentration of the untreated landfill gas while the gas emission is minimized. In experiments, the untreated landfill gas with different methane concentrations and flow rates is supplied to the combustor. Accordingly, the supply air is varied to proportionally yield different concentrations of oxygen, which is left in exhaust gas.

The suitable amount of supply air can be indicated by the oxygen concentration in exhaust air.

Figure 3.7 Testing combustor and data acquisition for optimal control design.

Figure 3.8 shows the plots of the measured variables of the combustion with respect to the oxygen concentrations in exhaust gas, such as the temperatures of exhaust gas, carbon monoxide concentration, and nitrogen oxide concentration at various methane concentrations. The left column and the right column present those combustion results with the different flow rates of the untreated landfill gas of 0.2 L/min and 0.1 L/min, respectively. In figure 3.8(a), the greater the methane concentration, the higher the temperature of exhaust gas, for a given oxygen concentration in exhaust gas. The higher temperature of exhaust gas can be established by the more concentration of methane gas for a given flow rate. Compared with figure 3.8(b), it is observed that the higher flow rate of the untreated landfill gas at a given methane concentration and oxygen concentration in exhaust gas causes the higher temperature of exhaust gas. In combustion control, the temperature of exhaust gas can be adjusted effectively to be higher or lower than previous operating temperatures by regulating the flow rate of the untreated landfill gas, even it is enhanced with the high concentration of methane gas. The trend lines at a given methane concentration of the untreated landfill gas are considered from figure 3.8(a) to figure 3.8(f) as follows. In figure 3.8(a) and figure 3.8(b), the temperature of exhaust gas increases as the oxygen concentration in exhaust gas increases. This situation is expected since the supply air can be used to burn the remaining methane gas in the combustor. After the highest point, the temperature of exhaust gas decreases as the oxygen concentration in exhaust gas increases. This result can be explained from no remaining methane gas in exhaust gas and excessive supply air to cool the exhaust gas down. In figure 3.8(c) and figure 3.8(d), the nitrogen oxide concentration increases as the oxygen concentration in exhaust gas increases since the availability of excessive oxygen gas is good at reaction to nitrogen gas. On the other hand, the carbon monoxide concentration decreases as the oxygen concentration in exhaust gas increases, as illustrated in figure 3.8(e) and figure 3.8(f). The excessive oxygen gas is capable of reacting with carbon monoxide to be carbon dioxide according to Eq. (3.3).

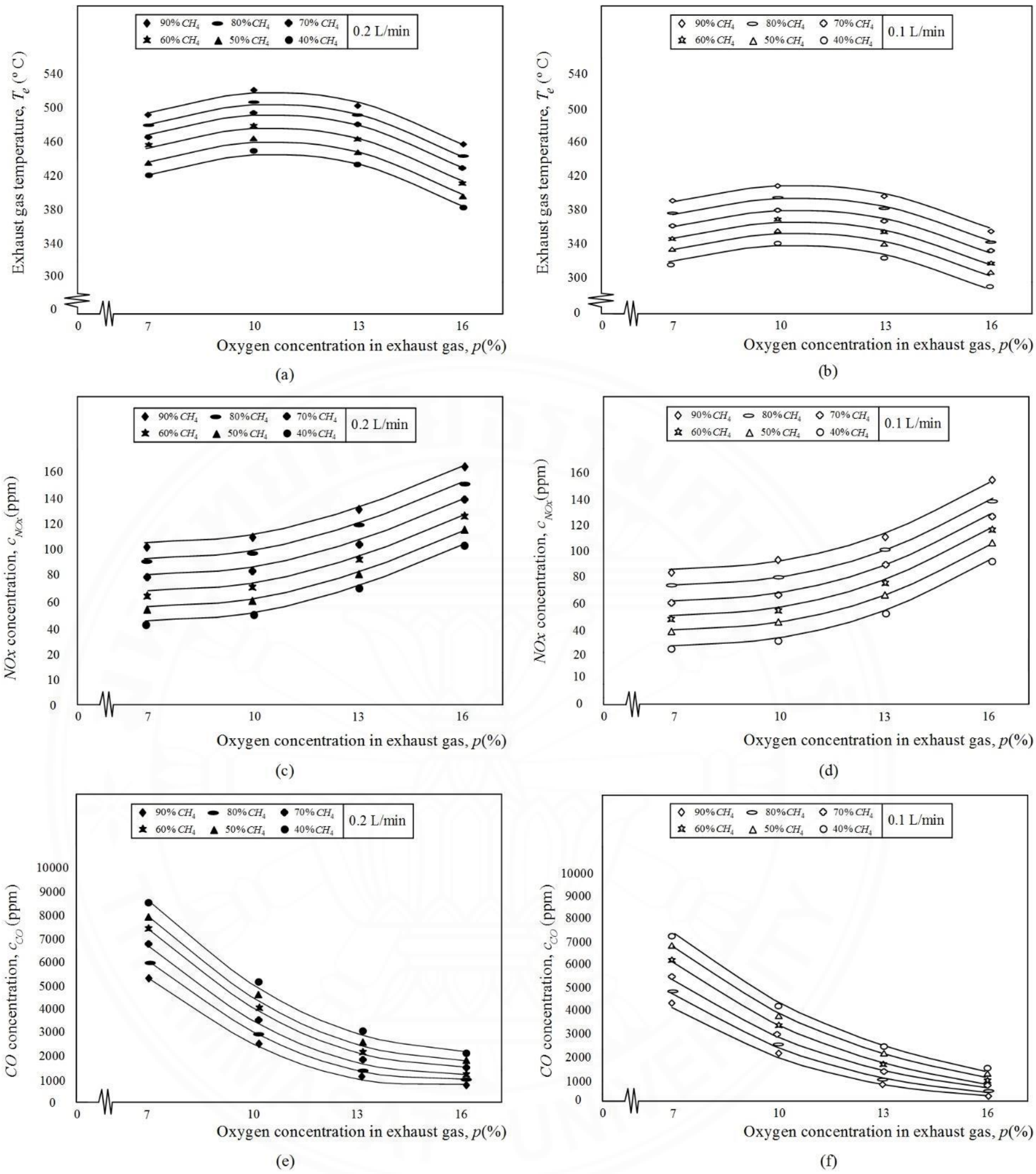

Figure 3.8 Experimental results of combustion with various methane concentration: (a) exhaust gas temperature at 0.2 L/min, (b) exhaust gas temperature at 0.1 L/min, (c) nitrogen oxide concentration at 0.2 L/min, (d) nitrogen oxide concentration at 0.1 L/min, (e) carbon monoxide concentration at 0.2 L/min, (f) carbon monoxide concentration at 0.1 L/min.

It can be interpreted that the peak points are located with inherent behaviors of the combustor. Those indeterminate characteristics of combustion cannot be found from an analytical work but from an actual experiment, which is proposed to be done in this study. From the implication of figure 3.8, the oxygen concentration in exhaust gas can be used as the design variable to indicate the combustion performance to obtain the most thermal efficiency and emission reduction, as proposed in Eq. (3.6). In this work, the performance index is expressed as:

$$PI = w_T \left(\frac{T_e}{T_{e,max}}\right)^2 + w_{co} \left(\frac{1}{c_{co}/c_{co,max}}\right)^2 + w_{NOx} \left(\frac{1}{c_{NOx}/c_{NOx,max}}\right)^2 \tag{3.6}$$

where $T_{e,max}$ is the maximum exhaust gas temperature at the same flow rate and methane concentration of the untreated landfill gas, $c_{co,max}$ is the maximum carbon monoxide concentration at the same flow rate and methane concentration of the untreated landfill gas, and c_{NOx} is the maximum nitrogen oxide concentration at the same flow rate and methane concentration of the untreated landfill gas, and w is the weighting factor for normalizing. After the data plots of figure 3.8 are inputted to Eq. (3.6) with w_T = 0.947, w_{co} = 0.526x10^{-5}, and w_{NOx} = 0.657x10^{-2}, figure 3.9 is obtained to present the trend line of the performance index. It can be seen that the maximum performance index is found when the combustor is operated at the optimal oxygen concentration in exhaust gas of 10%. This value is used as the reference point of the oxygen concentration in regulating the supply air for optimal combustion control.

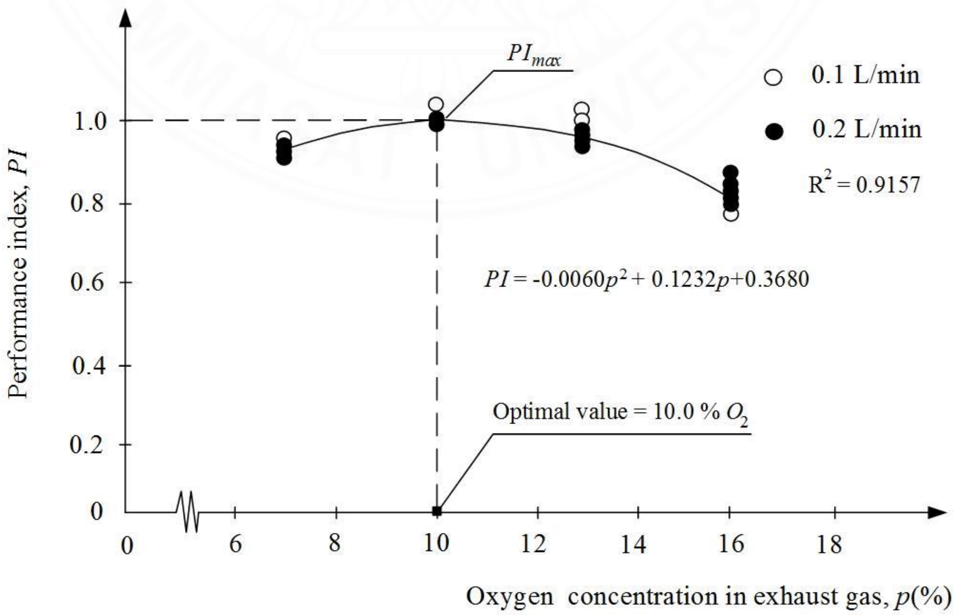

Figure 3.9 Plots of performance index against oxygen concentration in exhaust gas.

To demonstrate effectiveness of the proposed methodology, the experimental results in combustion of the untreated landfill gas is presented as figure 3.10. In figure 3.10(a), the methane concentration of untreated landfill gas changes from 60% to 50% around time of 10 s. Without control, the exhaust gas temperature decreases, accordingly, with the average error of 12.5 ºC, as seen figure 3.10(b), since there is less amount of methane gas in the untreated landfill gas. Correspondingly, the concentration of nitrogen oxide significantly increases by 28.50%, even though the concentration of carbon monoxide decreases by 18.75% at next steady state, as shown in figure 3.10(c), due to less methane gas and more supply air. However, figure 3.10(d) obviously indicates the decrease of performance index from the maximum value of unity to 0.94 by 6% over time after the concentration of methane gas decreases. It can be seen that the exhaust gas temperature is not maintained at the desired temperature and the gas emission is largely produced, when the methane concentration of untreated landfill gas is varied from the operating condition.

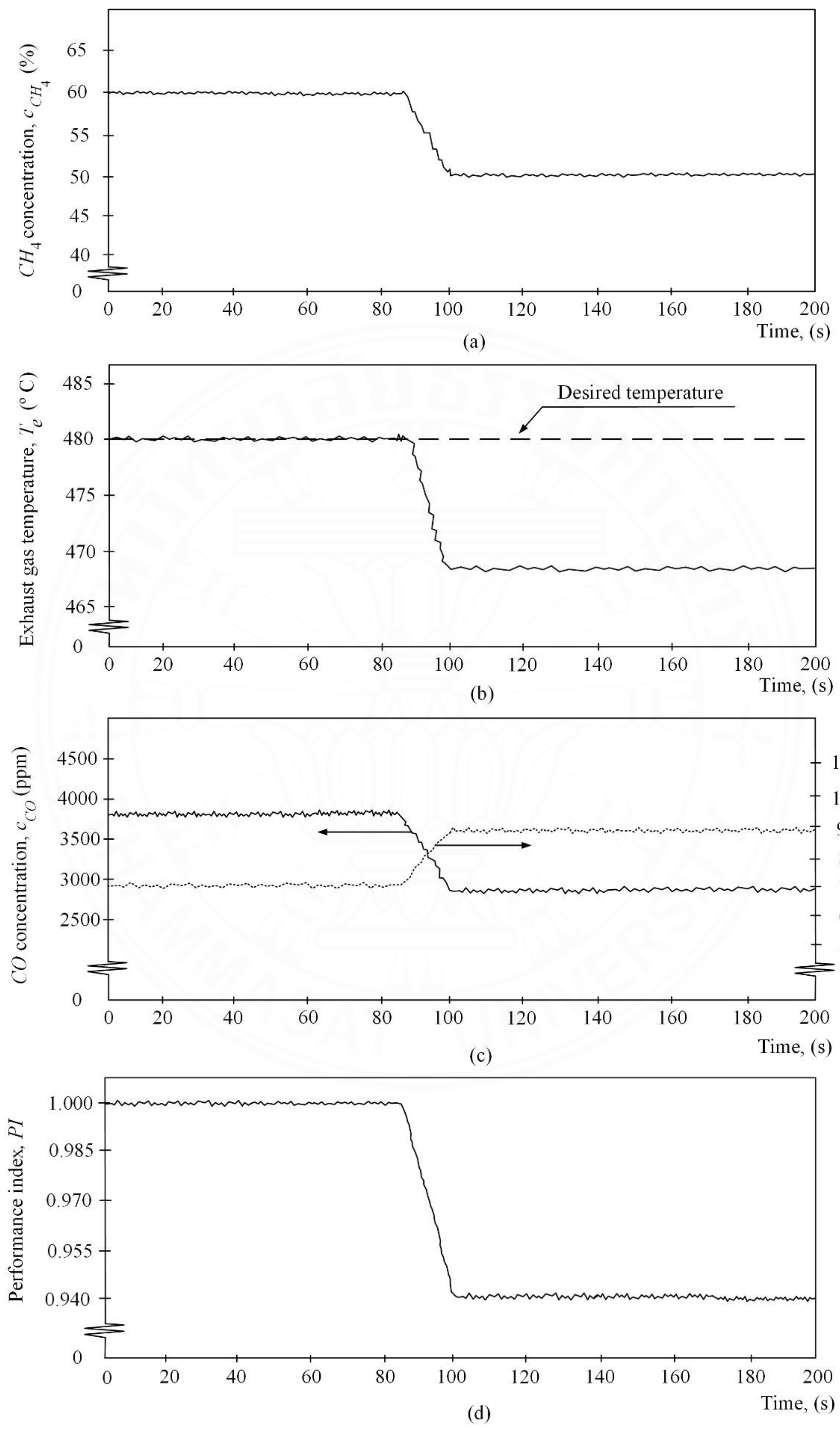

Figure 3.10 Performance of testing combustor without control.

To improve the combustion performance, the proposed methodology, as discussed in section, is applied to the combustor. The actual temperature of exhaust gas and the concentration of oxygen in exhaust gas are tightly controlled at the reference point and the optimal value of oxygen concentration in exhaust gas, respectively. In figure 3.1, two fuzzy logic control rules for the controllers of two flow control valves are defined as follows.

R1: If the error, e , is Negative, then the increasing percentage of open period, Δu , is Negative.

R2: If the error, e , is Zero, then the increasing percentage of open period, Δu , is Zero.

R3: If the error, e , is Positive, then the increasing percentage of open period, Δu , is Positive.

The fuzzy sets for control laws are defined according to membership functions, as depicted in figure 3.11. It should be remarked that the normal percentage of open period, u^*, is suggested to be 50% for wide range of increasing or decreasing flow rate.

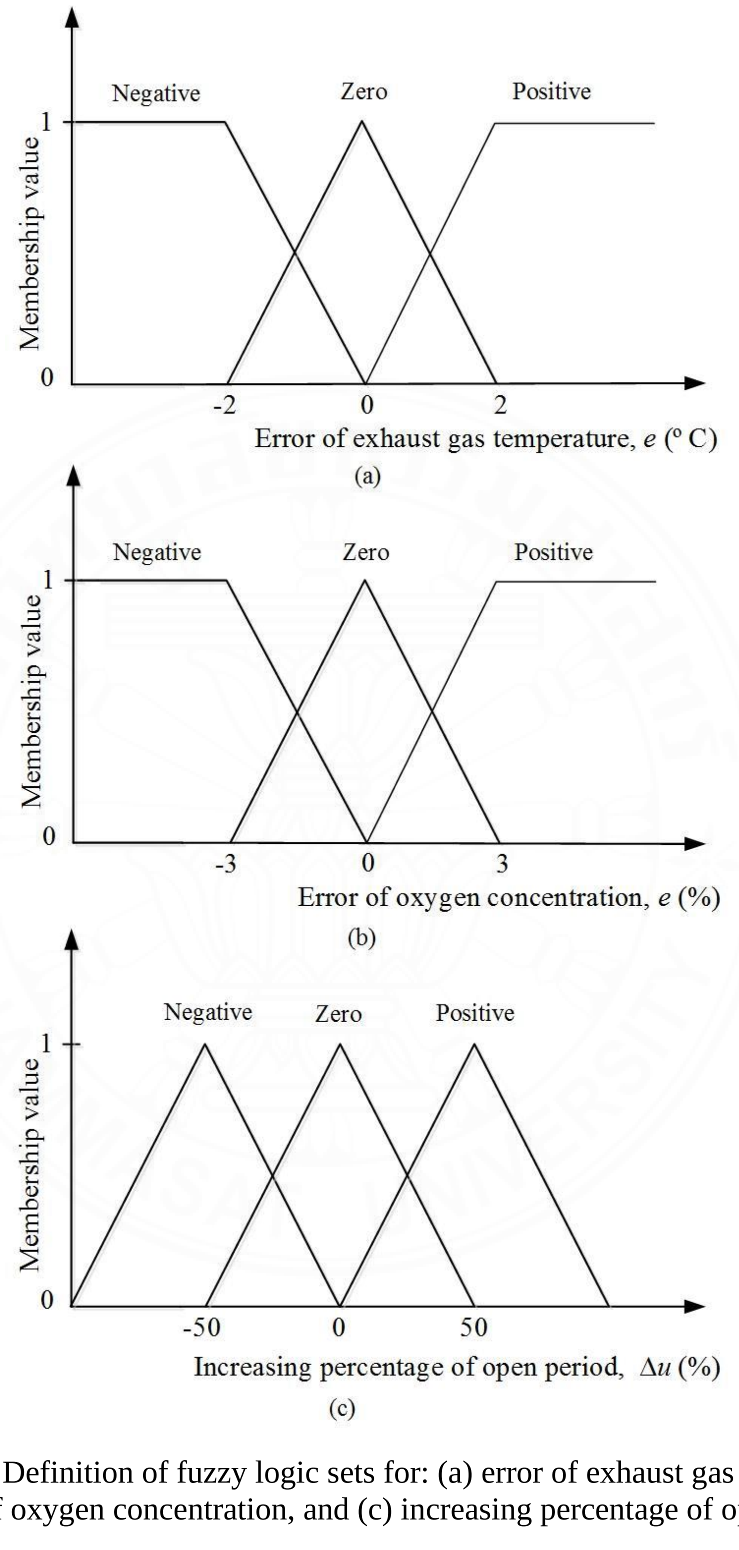

Figure 3.11 Definition of fuzzy logic sets for: (a) error of exhaust gas temperature, (b) error of oxygen concentration, and (c) increasing percentage of open period.

The flow rates of the untreated landfill gas and supply air are tightly managed via fuzzy logic based PWM regulation of flow control valves such a way that the errors between the reference points and actual values are eliminated over time. In fact, the number of fuzzy sets and parametric values can be subjectively defined from experiences. In this work, the error ranges of exhaust gas temperature and oxygen concentration in exhaust are intensively considered from -2 ºC to 2 ºC and from -3% to 3%, respectively. For example, the increasing percentage of open period is adjusted at the minimum magnitude of -50% when the error is less than -2 ºC or -3 %, as linguistically defined in figure 3.11. In turn, the percentage of open period is determined to be 0% for regulating the on/off switch of the flow control valves during the duty period. The null percentage of open period means switching off the flow control valves during that duty period. Also, the same consideration is extended for real-time control implementation when the errors are greater than 2 ºC or 3 % and between -2 12 ºC or -3 % and 2 ºC or 3 %. figure 3.12 shows the performance of combustion control in real time when the methane concentration of the untreated landfill gas is changed from 60% to 50% at time of 40 s, as depicted in figure 3.12(a) and the reference point of exhaust gas temperature is set from 480 ºC to 475 ºC at time of 120 s in sequence, as shown in figure 3.12(b). At time of 40 s, the exhaust gas temperature is expected to drop down due to less concentration of methane gas in the untreated landfill gas. As depicted in figure 3.12(c), a fuzzy logic controller immediately command to switch on the flow control valve of the untreated landfill gas further with increasing percentage of open period from 50% so that the exhaust gas temperature rises up and remains at the reference point of 480 ºC. Simultaneously, another fuzzy logic controller command to switch off the flow control valve of the supply air further with decreasing percentage of open period so that the oxygen concentration in exhaust gas reduces and remains at the reference point of 10%, as shown in figure 3.12(d). Afterward, two fuzzy logic controllers are capable of bringing the exhaust gas temperature and the oxygen concentration back to the reference points. Even though the reference point of exhaust gas temperature is altered from 480 ºC to 475 ºC at time of 120 s, two fuzzy logic controllers drive the exhaust gas temperature to the new reference point under maximizing the performance index at unity over time, as shown in figure 3.12(e). Those experimental results insist that the untreated landfill gas is optimally controlled in combustion to obtain the most thermal efficiency and gas-emission reduction via the proposed methodology of fuzzy logic rule knowledge based approach.

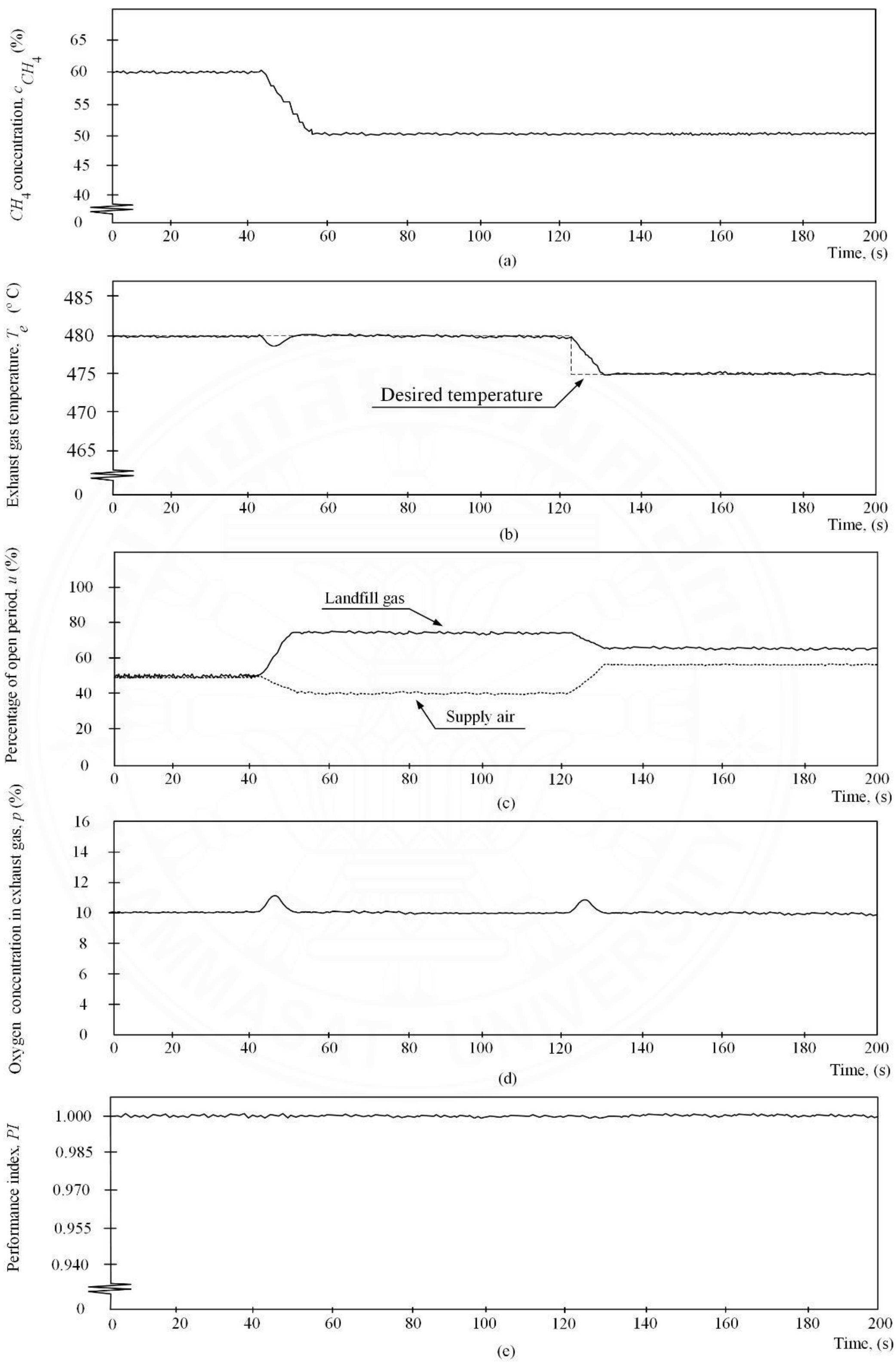

Figure 3.12 Performance of optimal combustion control via fuzzy logic rule knowledge based approach: (a) methane concentration, (b) exhaust gas temperature, (c) oxygen concentration in exhaust gas, (d) percentage of open period, and (e) performance index.

CHAPTER 4
CONCLUSIONS

4.1 Conclusions of feasibility analysis of power generation from landfill gas

The feasibility analysis of investment in electricity generation from landfill gas is performed with three types of power engines: ICE, ORC, and STE under current conditions of Thailand. The electricity generation of ICE from landfill gas is the most worth investment due to all satisfactory financial indices. Particularly, the values of $LCOE$ from ICE, ORC, and STE are determined to be 0.11USD / kWh, 0.30 USD/ kWh, 0.42 USD / kWh, respectively. The power engine ICE yields the lowest $LCOE$ among other power engines. The positive results of NPV, IRR, and PB confirms the most financial benefit to electricity generation of ICE from landfill gas. However, this result may change when the costs of imported ORC and STE decrease or some subsidies for financial incentive are provided from government.

4.2 Conclusions of sequential control of multichannel on–off valves

In the proposed methodology, multichannel on–off flow control valves in a parallel pattern are controlled by averaging PWM, which precisely regulates the volumetric flow rate with minimization of overflow and underflow during entire cycle periods. The averaging PWM yields overflow during the former half of the duty period and the latter half of the duty period after underflow. In turn, the overflow does not take a long time in one time within a single cycle period. The actual volumetric flow rate is able to closely track the required volumetric flow rate through a cycle period. Compared to the conventional PWM, the balanced flow control with the averaging PWM yields significantly less deviation of the process output close to the desired volumetric flow rate during the cycle period. The open/closed interval is set to be sampling time due to the shortest period of the valve responses while the number of the open/closed intervals within a cycle period is to be responsive to desired flow rates out of full flow rates. The empirical model of flow characteristics is used to determine the volumetric flow rate at full open positions under operating conditions. From the experimental results, the resolution of flow control can be improved by multichannel on–off valves. The sequential control of multichannel on–off valves yields the actual flow rate at given set points without a flow meter as observed in experiments. In general, the costs of pressure sensors and a temperature sensor are lower than a flow meter. Furthermore, there is no pressure drop due to those measurement devices. However, the number of on–off valves is chosen by tradeoff between cost and performance requirements. For installation, each flow control valve is straightforwardly added on to the valve module.

4.3 Conclusions of combustion control using fuzzy logic controller

The combustion control of untreated landfill gas with valves is difficult to obtain the desired exhaust gas temperature with maximum thermal efficiency and minimum gas emission under varying methane concentrations. Without control, it is observed that the exhaust gas temperatures are wildly deviated from the reference point during the combustion process over time, while gas emission is not minimized. For best practice, the most thermal efficiency is to maximize the exhaust gas temperature at the desired temperature for consuming a given flow rate and methane concentration of the untreated landfill gas, while gas emission of nitrogen oxide and carbon monoxide is minimized. In this work, the inherent performance index is defined from the experimental investigation on the combustor, which is considered for control. When it is maximized, the thermal efficiency is maximized and the gas emission is minimized. It is found that the oxygen concentration in exhaust gas can be used as a design indicator for optimization constraints. For this testing combustor, the oxygen concentration is to be maintained at 10% at the optimal point. The fuzzy logic rule knowledge based approach is implemented to regulate the flow rates of the untreated landfill gas and supply air so that the maximum value of performance index is obtained all the time. The proposed methodology can be generalized in optimal combustion control of untreated landfill gas via the fuzzy logic rule knowledge based approach, which is suitable to characteristics of each combustor.

4.4 Recommendation

From the experimental results of can-type combustor, it is confirmed that the optimal combustion of untreated landfill gas can achieve the desired exhaust gas temperature with maximum thermal efficiency and minimum gas emission by varying methane concentration or changing some operating conditions. This proposed methodology can be used generalize to control untreated landfill gas via fuzzy logic rule which is suitable for each combustor characteristics.

REFERENCES

Alemayehu, P. W., Pable, L.-S., Bejarano-Nosas, D., Teixeira-Dias, B., & Ioans, K. (2014). Electrochemically Actuated Passive Stop-Go Microvalves for Flow Control in Microfluidic Systems. *Microelectronic Engineering*, *111*, 416-420.

Aracil, C., Haro, P., Fuentes-Cano, D., & Gómez-Barea, A. (2018). Implementation of waste-to-energy options in landfill-dominated countries: Economic evaluation and GHG impact. *Waste Management*, *76*, 443-456.

Askari, M.H., & Ashjaee, M. (2017). Experimental measurement of laminar burning velocity and flammability limits of landfill gas at atmospheric and elevated Pressures. *Energy and Fuels*, *31*, 3196-3205.

Barth, E. J., Zhang, J., & Goldfarb, M. (2003). Control Design for Relative Stability in a PWM-Controlled Pneumatic System. *The American Society of Mechanical Engineers Journal of Dynamic Systems, Measurement, and Control*, *125*(3), 504-508.

Brett, M.-E., Shao, S., Stoia, J. L., & Eddington, D. T. (2011). Controlling Flow in Microfluidic Channels With a Manually Actuated Pin Valve. *Biomedical Microdevices*, *13*(4), 633–639.

Cheng, C.H., & Yang, H.S. (2012). Optimization of geometrical parameters for Stirling engines based on theoretical analysis. *Applied Energy*, *92*, 395-405.

Dino, C., Lawence, K., & Marc, M., (2015). A Novel Magnetic Active Valve for Lab-on-CD Technology. *Journal of Microelectromechanical Systems*, *24*(5), 1322–1330.

Eyidogan, M., Kilic, F.C., Kaya, D., Coban, V., & Cagman. S. (2016). Investigation of Organic Rankine Cycle (ORC) technologies in Turkey from the technical and economic point of view. *Renewable and Sustainable Energy Reviews*, *58*, 885- 895.

Gosieewski, K., Pawlaczyk, A., Warmuzinski, K., & Jaschik, M. (2009). A study on thermal combustion of leanmethane-air mixtures: Simplified reaction mechanism and kinetic equations. *Chemical Engineering Journal, 154*, 9-16.

Grebenkin, I., Muradov, K., & Davies, D. (2015). A Stochastic Approach for Evaluating Where on/Off Zonal Production Control Is Efficient. *Journal of Petroleum Science and Engineering, 132*, 28–38.

Hejrati, B., & Najafi, F. (2013). Accurate Pressure Control of a Pneumatic Actuator With a Novel Pulse Width Modulation-Sliding Mode Controller Using a Fast Switching on/Off Valve. *Proceedings of the Institution of Mechanical Engineers. Part I, Journal of Systems and Control Engineering, 227*(2), 230-242.

Hin Lai, A.C., & Keung Law, A.W. (2019). Numerical modeling of municipal waste bed incineration. *International Journal of Numerical Methods for Heat and Fluid Flow, 29*, 504-522.

Jerzak, W., Ku´znia, M., & Zajemska, M. (2014). The effect of adding $CO2$ to the axis of natural gas combustion flames on CO and NOX concentrations in the combustion chamber, *Journal of Power Technologies, 94*, 202-210.

Kong, X.Q., Wang, R.Z., & Huang. X.H. (2004). Energy efficiency and economic feasibility of CHP driven by stirling engine. *Energy Conversion and Management, 45*, 1433-1442.

Korkmaz, M., Ritter, D., Jochim, B., Beeckmann, J., Abel, D., & Heinz G. (2019). Effects of injection strategy on performance and emissions metrics in a diesel/methane dual-fuel single-cylinder compression ignition engine. *International Journal of Engine Research*.

Leephakpreeda, T. (1999). H_∞ Stability Robustness of Fuzzy Control Systems. *Automatica, 38*, 1467-1470.

Leephakpreeda, T. (2003). Flow-Sensorless Control Valve: Neural Computing Approach. *Flow Measurement and Instrumentation, 14*(6), 261-266.

Leephakpreeda, T. (2011). Fuzzy Logic Based PWM Control and Neural Controlled-Variable Estimation of Pneumatic Artificial Muscle Actuators. *Expert Systems with Applications, 38*(6), 7837-7850.

Li, J., Chou, S.K., Yang, W.M., & Li, Z.W. (2009). A numerical study on premixed micro combustion of $CH4$–air mixture:Effects of combustor size, geometry and boundary conditions on flame temperature. *Chemical Engineering Journal, 150*, 213-222.

Li, M., Zheng, X., Zhang, Q., Li, Z., Shen, B., & Liu, X. (2019). The effects of partially premixed combustion mode on the performance and emissions of a direct injection natural gas engine, *Fuel*, 218-234.

Lombardi, L., & Carnevale, E.A. (2016). Analysis of an innovative process for landfill gas quality improvement. *Energy, 109,* 1107-1117.

Maria, F.D., Micale, C., & Sordi, A. (2014). Electrical energy production from the integrated aerobic-anaerobic treatment of organic waste by ORC. *Renewable Energy, 66*, 461-467.

Mathis, W.J., & Ellzey, J.L. (2003). Flame stabilization operating range and emissions for a methane/air porous burner. *Combustion Science and Technology, 175*(5), 825-839.

Mercorelli, P. (2014). An Adaptive and Optimized Switching Observer for Sensorless Control of an Electromagnetic Valve Actuator in Camless Internal Combustion Engines. *Asian Journal of Control*, *16*(4), 959-973.

Mercorelli, P., & Werner, N. (2016). Integrating a Piezoelectric Actuator With Mechanical and Hydraulic Devices to Control Camless Engines. *Mechanical Systems and Signal Processing*, *78,* 55-70.

Mönkäre, T.J., Palmroth, M., Sormunen, K., & Rintala. J.A. (2019). Scaling up the treatment of the fine fraction from landfill mining: Mass balance and cost structure, *Journal of Waste Management*, *87*, 464-471.

Nguyen, T., Leavitt, J., Jabbari, F., & Bobrow, J. E. (2007). Accurate Sliding-Mode Control of Pneumatic Systems Using Low-Cost Solenoid Valves. *IEEE/ASME Transactions on Mechatronics*, *12*(2), 216–219.

Nuchkrua, T., & Leephakpreeda, T. (2013). Fuzzy Self-Tuning PID Control of Hydrogen-Driven Pneumatic Artificial Muscle Actuator. *Journal of Bionic Engineering, 10*, 329-340.

Nuchkrua, T., Leephakpreeda, T., & Chen, S. (2016). Experimental Validation for Fuzzy Control of Servo Pneumatic Artificial Muscle Driven by Metal Hydride. *International Journal of Fuzzy Systems, 18,* 956–970.

Pan, M., Johnston, N., Robertson, J., Andrew, P., Andrew, H., & Huayong, Y. (2015). Experimental Investigation of a Switched Inertance Hydraulic System With a High-Speed Rotary Valve. *The American Society of Mechanical Engineers Journal of Dynamic Systems, Measurement, and Control, 137*(12), 121003.

Pawananont, K., & Leephakpreeda, T. (2017). Feasibility analysis of power generation from landfill gas by using internal combustion engine, organic Rankine cycle and Stirling engine of pilot experiments in Thailand. *Energy Procedia, 138,* 575-579.

Pawananont, K., & Leephakpreeda, T. (2019). Sequential control of multichannel on-off valves for linear flow characteristics via averaging pulse width modulation without flow meter: An application for pneumatic valves. *Journal of Dynamic Systems, Measurement and Control, 141*(1).

Pawananont, K., & Leephakpreeda, T. (2021). Experimental investigation and optimal combustion control of untreated landfill gas via fuzzy logic rule knowledge based approach. *Journal of Waste Management, 121*, 383-392.

Pawlaczyk, A., & Gosiewski, K. (2015). Combustion of lean methane–air mixtures in monolith beds: Kinetic studies in low and high temperatures. *Chemical Engineering Journal, 282*, 29-36.

Pierpaoli, P., & Diotallevi, A. (2007). Generting Electrical Energy from Landfill Gas: an Italian Experience. *International Energy Journal, 8*, 45-50.

Quyen Minh, L., Mihn Tu, P., Mahdi, T., Richard, M., Jean-Pierre, S., & Tanneguy, R. (2013). Bilateral Control of Nonlinear Pneumatic Teleoperation System With Solenoid Valves. *IEEE Transactions on Control Systems Technology, 21*(4), 1463–1470.

Rannow, M. B., & Li, P. Y. (2012). Soft Switching Approach to Reducing Transition Losses in an on/Off Hydraulic Valve. *The American Society of Mechanical Engineers Journal of Dynamic Systems, Measurement, and Control, 134*(6), 064501.

Rendi, S.J., Houshfar, E., & Ashjaee, M. (2018). Combined experimental numerical investigation on the structure of methane/landfill gas flame using PIV. *Experimental Thermal and Fluid Science, 94*, 23-33.

Rentizelas, A., Karellas, S., Kakaras, E., & Tatsiopoulos, I. (2009). Comparative techno economic analysis of ORC and gasification for bioenergy applications. *Energy Conversion and Management*, *50,* 674-681.

Stamenic, M., Simonovic, T., & Tanasic, N. (2018). Efficient technology for combustion of low calorific gaseous fuels. *Proceedings of the 2018 5th International Symposium on Environment-Friendly Energies and Applications.* doi: 10.1109/EFEA.2018.8617090

Van Varseveld, R. B., & Bone, G. M. (1997). Accurate Position Control of a Pneumatic Actuator Using on/Off Solenoid Valves. *IEEE/ASME Transactions on Mechatronics*, *2*(3), 195–201.

Xue'en, Y., Alexander, H., Stuart A, J., Jeffrey H, L., Martin A, S., & Stephen D, U. (2004). An Electrostatic, on/Off Microvalve Designed for Gas Fuel Delivery for the MIT Microengine. *Journal of Microelectromechanical Systems*, *13*(4), 660–668.

Yucekaya, A. (2014). Landfill Gas to Energy in Turkey: Current and Future. *Journal of Science and Technology, 2,* 55-64.

Zeng, W., Liu, J., Ma, H., Liu, Y., & Liu, A. (2018). Experimental study on the flame propagation and laminar combustion characteristics of landfill gas. *Energy, 158,* 437- 448.

Zhao, X., Li, L., Song, J., Li, C., & Xian, G. (2016). Linear Control of Switching Valve in Vehicle Hydraulic Control Unit Based on Sensorless Solenoid Position Estimation. *IEEE Transactions on Industrial Electronics*, *63*(7), 4073-4085.

Zhu, K., Gu, L., Chen, Y., and Li, W. (2012). High Speed on/Off Valve Control Hydraulic Propeller. *Chinese Journal of Mechanical Engineering, 25*(3), 463-473.

APPENDICES

APPENDIX A
Pneumatic valves

This section presents the calculation for the number of open intervals for each flow control valve. It is supposed that $K = 8$, $n = 4$, and $p = 0.78$. Table 1 shows the numerical results, which are determined from Eq. (2.21).

It can be implemented in real time that the valves from channel 1 to channel 6 are fully open and the valve at the channel 8 is fully closed at a given cycle period. The valve at channel 7 is open for a first open/closed interval, and it is closed for all remaining three open/closed intervals. If the open/closed interval is 0.1 s, then the cycle period is 0.4 s. It is found that the resolution of the volumetric flow rate can be obtained to be 1/ (8 × 4) of the volumetric flow rate at full open positions of the flow control valves. Also, the integer of 25/32 is closer to 0.78 than 3/4 in the case that a single channel is applied.

Table A.1 Example of calculation for number of open intervals.

k	$\max\{(\text{int}(pnK)-(k-1)n),0\}$	$\min\{(\max\{(\text{int }(pnK)-(k-1)n),0\}), n\}$	h_k
1	25	4	4
2	21	4	4
3	17	4	4
4	13	4	4
5	9	4	4
6	5	4	4
7	1	1	1
8	0	0	0

APPENDIX B

I/O Connectors (myRIO Toolkit) for labview program

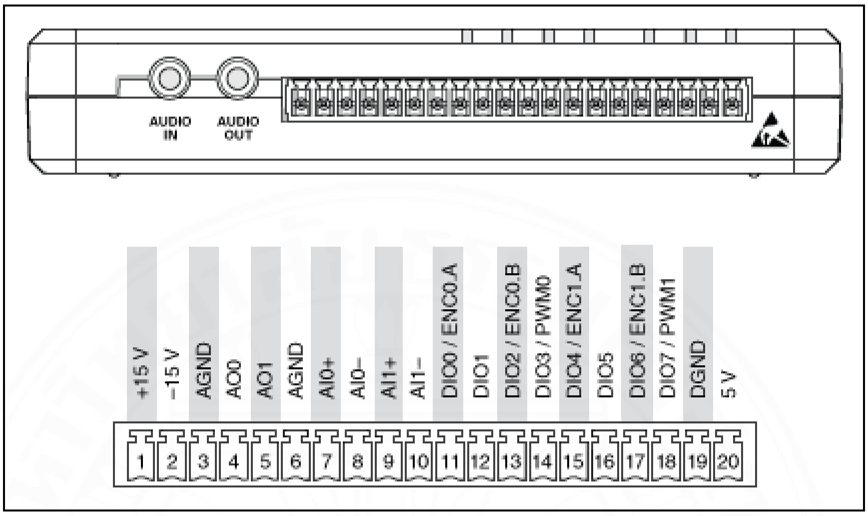

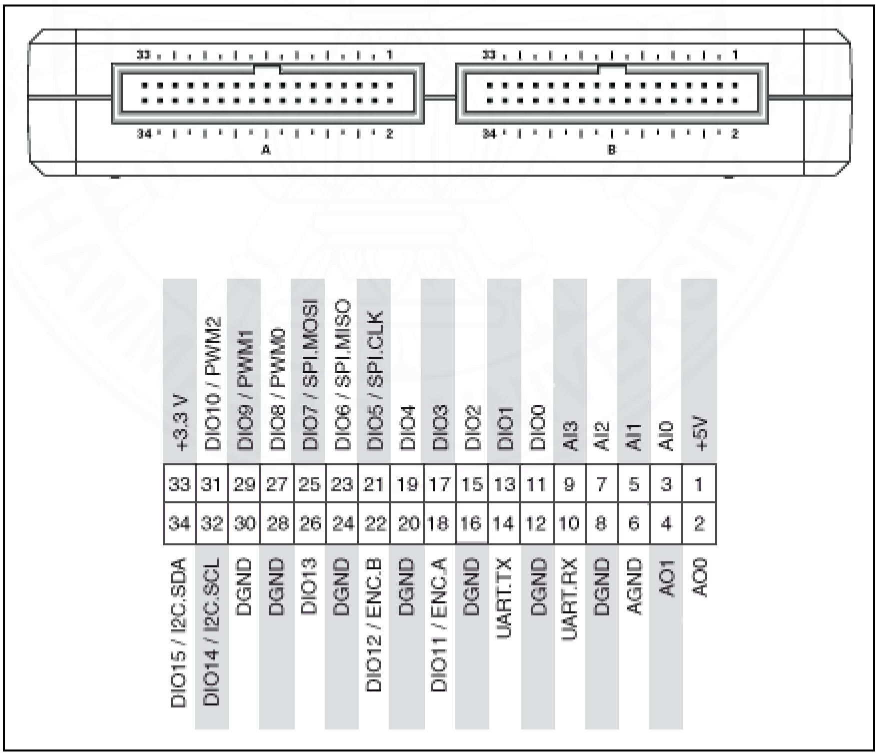

BIOGRAPHY

Name	Mr. Kanchit Pawananont
Date of Birth	August 9, 1981
Education	2005: Bachelor of Engineering (Electrical Engineering) Mahanakorn University of technology 2011: Master of Engineering (Control Engineering) King Mongkut's Institute of Technology Ladkrabang

Publications

Pawananont, K., & Leephakpreeda, T. (2017). Feasibility analysis of power generation from landfill gas by using internal combustion engine, organic Rankine cycle and Stirling engine of pilot experiments in Thailand. *Energy Procedia, 138,* 575-579.

Pawananont, K., & Leephakpreeda, T. (2019). Sequential control of multichannel on-off valves for linear flow characteristics via averaging pulse width modulation without flow meter: An application for pneumatic valves. *Journal of Dynamic Systems, Measurement and Control, 141*(1).

Pawananont, K., & Leephakpreeda, T. (2021). Experimental investigation and optimal combustion control of untreated landfill gas via fuzzy logic rule knowledge based approach. *Journal of Waste Management 121*, 383-392.